Acknowledgment. This research was supported by the U.S. National Science Foundation (Grant No. CHE 87-22561). Dr. John A. DiBenedetto, now at EG&G, Santa Barbara, made major contributions in the early stages of the research described in this manuscript. K.R.K. was the recipient of a University of California Special Regents Graduate Fellowship. We thank Professor R. J. Watts of this department for allowing the use of instrumentation for time-resolved spectral measurements and Christine Miller of this department for help in making such measurements. The contributions of Jerald A. Simon of this research group in modifying the computational hardware and software for excited-state lifetime measurements were incalculable.

Synthesis and Characterization of Macrobicyclic Iron(III) Sequestering Agents[1]

Thomas M. Garrett, Thomas J. McMurry, Mir Wais Hosseini, Zelideth E. Reyes, F. Ekkehardt Hahn, and Kenneth N. Raymond*

Contribution from the Department of Chemistry, University of California, Berkeley, California 94720. *Received February 12, 1990. Revised Manuscript Received October 16, 1990*

Abstract: This paper reports the template and high-dilution syntheses of a series of macrobicyclic iron(III) sequestering agents based on catechol as the ligating group. An X-ray structure of the salt denoted as Na_3[Fe(bicappedTRENCAM)]·17.5H_2O is the first for any ferric tricatechoyl amide and displays an unprecedented trigonal prismatic coordination (C_{3h} symmetry) for the ferric ion. The compound crystallizes in space group $P6_3/m$ with a = 13.785 (3) Å, c = 16.244 (5) Å, d_{obs} = 1.45, d_{calc} = 1.51 g cm^{-3}. The structure was refined to an R factor of 4.38, R_w = 5.16. The O–O atoms of the trigonal face are separated by 2.713 (3) Å, those related by the mirror plane by 2.526 (4) Å. The Fe–O distances are 2.012 (2) Å, and the bite angle is 77.75 (11)°. Solution thermodynamic studies on one of the ligands, bicappedTRENCAM, determine surprisingly low protonation constants (log K_1K_2 = 27.2 (1), log K_3 = 8.3 (1), log K_4K_5 = 8.73 (1), log $K_6K_7K_8$ = 9.75 (1)) containing a number of polyprotic steps. Aqueous electrochemical studies performed on the ferric complexes of these ligands show reversible reduction potentials of –0.89 to –0.97 V (vs NHE). While still highly selective for the ferric ion (ratios of the formation constants of ferric to ferrous complexes range from 28.1 to 29.5), these ligands have a slight stabilization of the ferrous complex relative to related tripodal compounds, one of which is the siderophore enterobactin. A slow protonation reaction is seen upon reduction of the ferric complexes. The protonation constant of the Fe(bicappedTRENCAM) complex proceeds in an unusual two-proton step with an equilibrium constant of (log K_1K_2) 10.65 (1). The complex formation constant (log K) is 43.1 (4), which shows no increase due to the macrobicyclic structure of the ligand relative to related hexadentate catechol ligands. The pM value is 30.7, where pM = –log [Fe] at pH 7.4 and $[Fe]_T = 10^{-6}$ M, $[L]_T = 10^{-5}$ M.

Introduction

The chemistry of metal ions in biological systems frequently shows remarkable specificity in complexing the targeted metal ion. The design of similar artificial sequestering agents, strongly and specifically to complex selected ions, has increasingly become an achievable goal. Thus, polyether and polyamine sequestering agents, with cyclic and bicyclic topologies, have produced metal complexes with unprecedented kinetic and thermodynamic stabilities.[2,3] Since nature has chosen the catechol ligand as the functional group in enterobactin, the siderophore which has the highest binding constant of these microbial iron binding agents,[4,5] we have selected catechol as the ligand to incorporate into a number of multidentate agents.[6,7] Introduction of the macrobicyclic framework into iron(III) sequestering agents was performed to see if similar increases in complexing ability could be achieved. The foremost feature of a macrobicyclic ligand is thermodynamic advantage, relative to less organized ligands.[8] Preorganizing the iron binding site should result in a higher formation constant. It should also produce a kinetically more stable complex[9] and result in markedly slower ligand exchange rates. In the limiting case it may be possible to produce an "inert" complex of high-spin Fe(III), a classic labile metal ion. Finally, the anticipated properties of these ligands suggest their potential use as pharmaceutical agents in ion decorporation or other sequestration applications.

In earlier catechol ligands we have incorporated 2,3-dihydroxyterephthalic acid, initially by using only one carboxylate group for attachment via an amide bond, with the remaining group used as a charged substituent to increase water solubility. More recently the research group of Vögtle[10,11] as well as we[12-14] have used both points of attachment of the 2,3-dihydroxyterephthalamide subunit (Figure 1) for macrocycle formation. We have recently shown that this subunit binds Fe(III) more strongly at physiological pH than any other bidentate chelate.[15] Thus it might

* To whom correspondence should be addressed.

(1) Paper no. 22 in the series Ferric Ion Sequestering Agents. For the previous paper in this series, see: Ng, C. Y.; Rodgers, S. J.; Raymond, K. N. *Inorg. Chem.* **1989**, *28*, 2062.
(2) Lehn, J.-M. *Science* **1985**, *227*, 849.
(3) Creaser, I. I.; Geue, R. J.; Harrowfield, J. MacB; Hertl, A. J.; Sargeson, A. M.; Snow, M. R.; Springborg, J. *J. Am. Chem. Soc.* **1982**, *104*, 6016. Geue, R. J.; Hambly, T. W.; Harrowfield, J. MacB.; Sargeson, A. M.; Snow, M. R. *J. Am. Chem. Soc.* **1984**, *106*, 5748.
(4) Matzanke, B. F.; Müller-Matzanke, G.; Raymond, K. N. *Iron Carriers and Iron Proteins*; Loehr, T. M., Ed.; Physical Bioinorganic Chemistry Series, VCH Publishers: New York, 1989; p 1.
(5) Raymond, K. N.; Müller, G.; Matzanke, B. F. *Top. Curr. Chem.* **1984**, *123*, 50.
(6) Raymond, K. N.; McMurry, T. J.; Garrett, T. M. *Pure Appl. Chem.* **1988**, *60*, 545.
(7) Raymond, K. N. *Environmental Inorganic Chemistry*; Irgolic, K. J., Martell, A. E., Eds.; VCH Publishers: Deerfield Beach, FL, 1985; p 331.
(8) Cram, D. J. *Angew. Chem., Int. Ed. Engl.* **1986**, *25*, 1039.
(9) Busch, D. H.; farmery, K.; Goedken, V.; Katovic, V.; Melnyk, A. C.; Sperati, C. R.; Tokel, N. *Advances in Chemistry Series*; Gould, R. F., Ed.; American Chemical Society: Washington, DC, 1971; Vol. 100, p 44.
(10) Kiggen, W.; Vögtle, F. *Angew. Chem., Int. Ed. Engl.* **1984**, *23*, 714.
(11) Stutte, P.; Kiggen, W.; Vögtle, F. *Tetrahedron* **1987**, *43*, 2065.
(12) Rodgers, S. J.; Ng, C. Y.; Raymond, K. N. *J. Am. Chem. Soc.* **1985**, *107*, 4094.
(13) McMurry, T. J.; Rodgers, S. J.; Raymond, K. N. *J. Am. Chem. Soc.* **1987**, *109*, 3451.
(14) McMurry, T. J.; Hosseini, M. W.; Garrett, T. M.; Hahn, F. E.; Reyes, Z. E.; Raymond, K. N. *J. Am. Chem. Soc.* **1987**, *109*, 7196.

0002-7863/91/1513-2965$02.50/0

be expected that the combination of increased enthalpic driving force as well as the lessening of required reorganization entropy would provide a ligand that is a stronger iron chelating agent than enterobactin. Indeed, Vögtle and co-workers[11] have reported a preliminary formation constant of 10^{59} for their mesitylene-based bicapped macrobicycle. As we will show, this estimate appears to be 16 orders of magnitude larger than the actual formation constants of these compounds. This paper will also report new routes to the synthesis of these macrobicyclic iron sequestering agents, their electrochemistry, solution thermodynamics, and structural characterization.

Experimental Section

Materials and Equipment. Thionyl chloride was purified by distillation from triphenyl phosphite. Tetrahydrofuran was distilled from sodium benzophenone ketyl. The amine TREN[16] was purified by distillation from sodium. Dioxane was refluxed over Na and distilled under argon. Dimethylformamide was predried with neutral alumina and vacuum distilled, discarding the first 10%, and stored over 4Å molecular sieves; DMSO (Burdick and Jackson) was refluxed over CaH_2, vacuum distilled, and stored over 4Å molecular sieves. Triethylamine was distilled from Na under argon. All other compounds used (except for water used in titrations, vide infra) were of reagent grade and were not further purified. Spectra were collected on a custom-built 200 MHz FT spectrometer (NMR) and a Nicolet 5/DX FT spectrometer (IR). Melting points were taken on a Büchi apparatus and are uncorrected. Analytical HPLC was performed on a Beckman 344 system equipped with a UV-vis detector, while preparative separations were achieved by using a Rainin Autoprep Gradient HPLC system. Microanalyses were performed by the Analytical Services Laboratory, College of Chemistry, University of California, Berkeley. Mass spectra were taken by the Mass Spectrometry Laboratory, College of Chemistry, University of California, Berkeley. Microprobe analysis was performed by the Electron Microprobe Laboratory, Department of Geology and Geophysics, University of California, Berkeley.

Synthesis. The starting material **1** was prepared by literature methods[17,18] in five steps and 17% overall yield. TPT was prepared by literature methods.[19] The starting material for the mesitylenetriamine synthesis, **16**, was produced in two steps and 57% overall yield by literature methods[20] from commercially available starting material. The starting material, dimethyl 2,3-dihydroxyterephthalate, was synthesized by literature methods in two steps and 66% overall yield.[17]

Compounds Prepared via Scheme I.[21] **2 (Scheme I).** In a 500-mL flask, 2.167 g (14.8 mmol, 1 equiv) of $N(CH_2CH_2NH_2)_3$, 200 mL of THF, and 18.59 mL of Et_3N were stirred under argon at room temperature. To this was added a solution of **1** (11.50 g, 44.5 mmol, 3 equiv) in 100 mL of THF dropwise over a period of 1 h, and the mixture was stirred for another 2–3 h. The solid Et_3NHCl was removed by filtration and washed with 3 × 30 mL of THF. The THF layers were combined and evaporated to dryness. The orange residue was heated to 60 °C and dried under vacuum. Pure Me_9TRENCAM-C was obtained after silica chromatography (4.3 × 40 cm gravity column, Davisil 62 60–200 mesh silica, 0–3% $MeOH/CH_2Cl_2$): R_f (5% $MeOH/CH_2Cl_2$) 0.24; yield 9.63 g (80%); ^1H NMR ($CDCl_3$) δ 8.08 (br t, 3 H, ARCONHR), 7.59 (d, 3 H, ArH), 7.39 (d, 3 H, ArH), 3.85 (s, 9 H, $ArOCH_3$), 3.83 (s, 9 H, $ArOCH_3$), 3.78 (s, 9 H, RCO_2CH_3), 3.52 (m, 6 H, $NCH_2CH_2NHCOAr$), 2.80 (t, 6 H, $NCH_2CH_2NHCOAr$); ^{13}C NMR ($CDCl_3$) δ 165.5, 164.4, 153.0, 152.1, 130.3, 128.7, 125.6, 125.3, 61.6, 53.4, 52.3, 37.8; IR (KBr pellet) 1735, 1651 cm^{-1}; mass spectrum (CI) 813 (M + H^+). Anal. Calcd for $C_{39}H_{48}N_4O_{15}\cdot CH_3OH$ (Found): C, 56.86 (56.32); H, 6.20 (5.91); N, 6.63 (6.71).

4 (Scheme I). To 2.0 g (2.46 mmol) in 30 mL of MeOH under N_2 was added 34 mL of 0.5 M NaOH (7 equiv). The solution was heated at reflux for 4 h and cooled to room temperature in an ice bath. The pH was lowered to 4 by slow addition, with frequent testing, of 10% HCl. The solution was evaporated with no heat applied. The yellowish oil was taken up in approximately 150 mL of 1:1 EtOH/MeOH and 6 drops of 10% HCl. This solution was filtered to remove NaCl and then evaporated. The white foam was evaporated two times from 50 mL of MeOH and dried under high vacuum with no heat: yield 2 g (100%); ^1H NMR (DMSO) δ 8.7 (br s, 3 H, CONH), 7.4 (br s, 6 H, ArH), 3.75 (m, 24 H, OCH_3 and CH_2NCO), 3.5 (br s, 6 H, CH_2N); ^{13}C NMR (DMSO) δ 166.71, 165.46, 132.47, 129.7, 124.61, 124.00, 51.94, 34.28; IR (KBr pellet) 1721, 1651 cm^{-1}; mass spectrum (FAB, glycerol–thioglycerol) 771 (M + H^+). Anal. Calcd for $C_{36}H_{42}N_4O_{15}\cdot HCl\cdot H_2O$ (Found): C, 52.39 (52.92); H, 5.50 (5.56); N, 6.79 (6.77).

5 (Scheme I). To 100 mg of **4**·HCl (0.121 mmol) in 30 mL of freshly distilled THF, under N_2, was added by Teflon cannula 0.06 mL of $SOCl_2$. The white slurry was let stir, whereupon a slightly yellow solution resulted. The acid chloride was used as the crude solution: IR (THF solution) 1778, 1654 cm^{-1}.

3 (Scheme I). R_f (10% $MeOH/CH_2Cl_2$) 0.50; yield 7.99 g (88%); ^1H NMR ($CDCl_3$) δ 8.04 (br t, 3 H, Arconhr), 7.61 (d, 3 H, ArH), 7.43 (d, 3 H, ArH), 3.85 (s, 9 H, $ArOCH_3$), 3.83 (s, 9 H, $ArOCH_3$), 3.81 (s, 9 H, CO_2CH_3), 3.44 (m, 6 H, $NCH_2CH_2CH_2NHCO$), 2.47 (t, 6 H, $NCH_2CH_2CH_2NHCO$), 1.71 (m, 6 H, $NCH_2CH_2CH_2NHCO$); ^{13}C NMR ($CDCl_3$) δ 165.6, 164.3, 153.1, 152.0, 130.9, 128.6, 125.7, 125.4, 61.7, 61.6, 52.3, 51.5, 38.1, 27.1; IR (KBr pellet) 1735, 1651 cm^{-1}; mass spectrum (CI) 855 (M + H^+), 823 (M + H^+ – OCH_3), 590 (M + H^+ – 1 cat). Anal. Calcd for $C_{42}H_{54}N_4O_{15}\cdot 2CH_3OH$ (Found): C, 57.50 (57.48); H, 6.80 (6.41); N, 6.09 (6.36).

6 (Scheme I): yield 2.49 g (94%); ^1H NMR (CD_3OD) δ 7.50 (m, 6 H, ArH), 3.93 (s, 9 H, $ArOCH_3$), 3.89 (s, 9 H, $ArOCH_3$), 3.58 (m, 6 H, $NCH_2CH_2CH_2NHCO$), 3.37 (m, 6 H, $NCH_2CH_2CH_2NHCO$), 2.11 (m, 6 H, $NCH_2CH_2CH_2NHCO$); IR (KBr pellet) 1728, 1658 cm^{-1}; mass spectrum (FAB, glycerol–thioglycerol) 813 (M + H^+). Anal. Calcd for $C_{39}H_{49}N_4O_{15}Cl\cdot HCL\cdot H_2O$ (Found): C, 51.28 (52.26); H, 6.14 (6.10); N, 6.20 (5.85).

7 (Scheme I): IR (KBr pellet) 1778, 1658 cm^{-1}.

Me_6bicappedTRENMECAM (8) (Scheme I). In a 2-L, three-necked flask, 1 L of THF was stirred mechanically under argon. To this was added simultaneously a solution of the acid chloride **5** (1 g, 1.2 mmol, 1 equiv in 250 mL of THF) and a solution of mesitylenetriamine (0.24 g, 1.45 mmol, 1.2 equiv) with 1.01 mL of Et_3N (7.25 mmol, 6 equiv) in 249 mL of THF) over a period of 6–7 h. The reaction mixture was allowed to stand 14 h. The precipitate was removed by filtration, and the solvent was evaporated to dryness. The crude product was chromatographed on silica (4.3 × 40 cm gravity column, Davisil 62 60–200 mesh silica, 0–5% $MeOH/CHCl_3$): R_f (10% $MeOH/CH_2Cl_2$) = 0.36. Evaporation of solvent gave a crystalline solid which was recrystallized from $CHCl_3/Et_2O$: yield 0.106 g (10%); ^1H NMR ($CDCl_3$) δ 7.70 (m, 6 H, ArCONH), 7.63 (q, 6 H, ArH), 7.50 (s, 3 H, ArH), 4.54 (d, 6 H, $HNCH_2Ar$), 3.68 (m, 6 H, NCH_2CH_2NHCO), 3.46 (s, 9 H, $ArOCH_3$), 2.92 (s, 9 H, $ArOCH_3$), 2.74 (br t, 6 H, NCH_2CH_2NHCO); ^{13}C NMR ($CDCl_3$) δ 165.0, 163.7, 151.4, 151.2, 141.6, 130.6 130.3, 128.9, 126.6, 125.9, 62.0, 61.0, 53.0, 44.0, 36.8; IR (KBr pellet) 1651 cm^{-1}; mass spectrum (FAB, glycerol–thioglycerol) 882 (M + H^+). Anal. Calcd for $C_{45}H_{51}N_7O_{12}\cdot{}^3/_4CHCl_3$ (Found): C, 56.56 (56.63); H, 5.38 (5.42); N, 10.09 (10.10).

BicappedTRENMECAM (12) (Scheme I). To 0.1 g of Me_6bicappedTRENMECAM (0.113 mmol, 1 equiv), under an N_2 atmosphere, was added 20 mL of dry $CHCl_3$, with stirring, and the starting material slowly dissolved. The reaction flask was immersed in an ice bath, and 0.75 mL (7.9 mmol, 70 equiv) of BBr_3 was added by Pasteur pipet under N_2 flush. A yellow precipitate formed, the ice bath was removed, and the slurry was stirred overnight. The reaction flask was again immersed in an ice bath, fitted with a condenser, and opened to the atmosphere. As MeOH was added dropwise in portions, a vigorous reaction developed; MeOH was added until the reaction subsided, about 30 mL of MeOH total. The ice bath was removed (the precipitate had dissolved), and the solution was stirred for 10 min. The solvent was then evaporated away. The light brown crude product was taken up in hot MeOH, and the solvent was evaporated away. This coevaporation was repeated nine more times. The resultant oil was then coevaporated with benzene four times, dissolved in MeOH, and precipitated with Et_2O, mp = 275–277 °C: yield 0.066 g (67%); ^1H NMR (CD_3OD, CD_3COCD_3) δ 7.5 (s, 3 H, ArH), 6.6 (br d, 3 H, ArH), 6.3 (br d, 3 H, ArH), 4.5 (s, 6 H, $ArCH_2NHCO$), 4.0 (br s, 6 H, NCH_2CH_2NHCO), 3.8 (br s, 6 H, NCH_2CH_2NHCO); mass spectrum (FAB, glycerol–thioglycerol) 798 (M

(15) Garrett, T. M.; Miller, P. W.; Raymond, K. N. *Inorg. Chem.* **1989**, *28*, 128.

(16) Abbreviations used in the text include the following: TREN, tris(2-aminoethyl)amine; TPT, 3,3′,3″-tris(aminopropyl)amine; FT, Fourier, transform; CI, chemical ionization; FAB, fast atom bombardment; THF, tetrahydrofuran; DMF, *N,N*-dimethylformamide; SCE, saturated calomel electrode; NHE, normal hydrogen electrode; DPP, differential pulse polarography, NPP, normal pulse polarography; *n*, number of electrons transferred; *m*, number of protons transferred; E_p, peak potential, $E^{o\prime}$, formal potential; *i*, current; CDTA, *trans*-1,2-cyclohexylenedinitrilotetraacetic acid; *R*, $[\sum(Y_o - Y_c)^2/\sum Y_o^2]^{1/2}$ where *Y* is the dependent variable; GOF, goodness-of-fit = $[\sum(Y_o - Y_c)^2/(N_{obs} - N_{var})]$; K_f, formation constant; MHz, megahertz; s, singlet; d, doublet; t, triplet; q, quintet; m, multiplet; br, broad.

(17) Weitl, F. L.; Raymond, K. N.; Durbin, P. W. *J. Med. Chem.* **1981**, *24*, 203.

(18) Rodgers, S. J. Ph.D. Dissertation, University of California, Berkeley, 1985.

(19) Dietrich, B.; Hosseini, M. W.; Lehn, J.-M.; Sessions, R. B. *Helv. Chim. Acta* **1985**, *68*, 289.

(20) Cochrane, W. P.; Pauson, P. L.; Stevens, T. S. *J. Chem. Soc. C* **1968**, 630.

Scheme I. Synthetic Route for Macrobicyclic Iron(III) Sequestering Agents

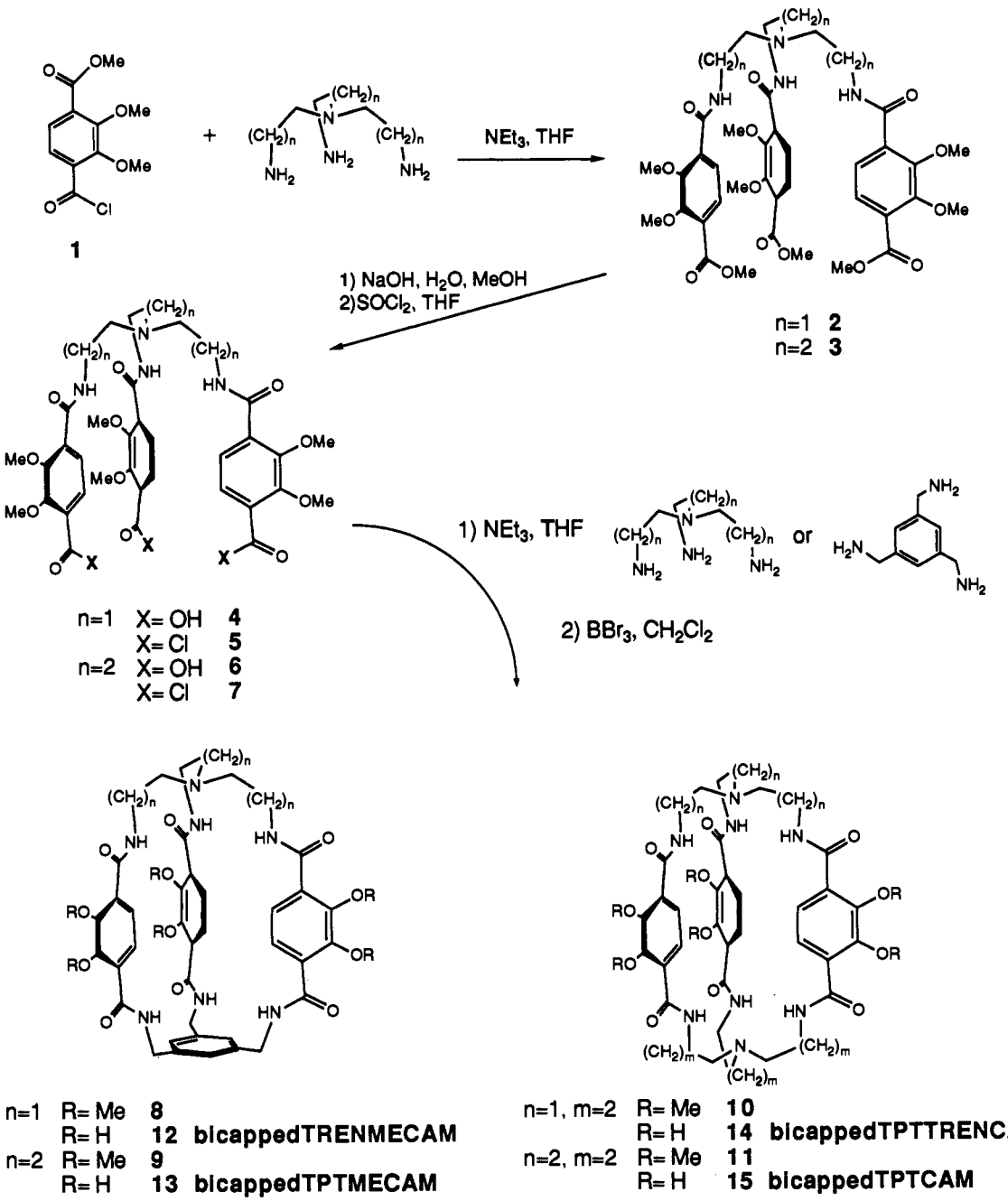

+ H^+); high-resolution mass calcd for $C_{39}H_{40}N_7O_{12}$ (found) 798.274 (798.271). Anal. Calcd for $C_{39}H_{39}N_7O_{12}\cdot 1.75HBr\cdot 0.5\ DMF\cdot 3H_2O$[21] (Found): C, 47.22 (47.03); H, 4.93 (4.65); N, 10.20 (10.11); Br, 13.57 (13.51).

Me_6bicappedTPTMECAM (9) (Scheme I): R_f (30% MeOH/CH_2Cl_2) = 0.47. Evaporation of the solvent gave a crystalline solid which was recrystallized from $CHCl_3/Et_2O$: yield 0.130 g (13%); ^1H NMR ($CDCl_3$) δ 8.07 (m, 6 H, ArCONH), 7.80 (m, 6 H, ArH), 7.49 (s, 3 H, ArH), 4.55 (d, 6 H, $NHCH_2Ar$), 3.54 (br s, 6 H, $NCH_2CH_2CH_2NHCO$), 3.52 (s, 9 H, $ArOCH_3$), 3.49 (s, 9 H, $ArOCH_3$), 2.65 (br s, 6 H, $NCH_2CH_2CH_2NHCO$), 1.84 (br s, $NCH_2CH_2CH_2NHCO$); ^{13}C NMR ($CDCl_3$) δ 163.4, 162.6, 150.8, 140.4, 129.4, 129.1, 128.7, 125.8, 60.9, 60.5, 51.0, 43.3, 37.6, 24.9; IR (KBr pellet) 1651 cm^{-1}; mass spectrum (FAB, glycerol–thioglycerol) 924 (M + H^+).

BicappedTPTMECAM (13) (Later Steps in Scheme I). The crude product was taken up in DMF and precipitated with Et_2O. The flocculent white solid was filtered on a 0.45 μm nylon filter and dried under vacuum, mp = 225 °C: yield 0.059 g (52%); ^1H NMR (DMSO-d_6) δ 9.0 (br s, 3 H, ArCONH), 8.6 (br s, 3 H, ArCONH), 7.4 (s, 3 H, ArH), 7.15 (br s, 6 H, ArH), 4.4 (br s, 6 H, $ArCH_2NHCO$), 3.4 (br s, 6 H, $NCH_2CH_2CH_2NHCO$), 2.75 (br s, 6 H, $NCH_2CH_2CH_2NHCO$), 1.8 (br s, 6 H, $NCH_2CH_2CH_2NHCO$); mass spectrum (FAB, glycerol–thioglycerol) 840 (M + H^+); high-resolution mass calcd for $C_{42}H_{46}N_7O_{12}$ (found) 840.320 (840.322). Anal. Calcd for $C_{42}H_{45}N_7O_{12}\cdot HBr\cdot DMF\cdot 3H_2O$ (Found): C, 51.57 (51.93); H, 5.69 (5.28); N, 10.69 (10.99).

Me_6bicappedTPTTRENCAM (10) (Scheme I): R_f (30% MeOH/CH_2Cl_2) 0.30. Evaporation of the solvent gave a crystalline solid: yield 0.122 g (11%); ^1H NMR ($CDCl_3$) δ 8.03 (br d, 6 H, ArCONH), 7.42 (d, 3 H, ArH), 7.31 (d, 3 H, ArH), 3.64 (s, 9 H, $ArOCH_3$), 3.60 (br s, 12 H, $ArCONHCH_2CH_2R$), 3.43 (s, 9 H, $ArOCH_3$), 2.77 (br s, 6 H, NCH_2CH_2NHCO), 2.64 (m, 6 H, $NCH_2CH_2CH_2NHCO$), 1.78 (br s, 6 H, $NCH_2CH_2CH_2NHCO$); ^{13}C NMR ($CDCl_3$) δ 165.5, 164.3, 150.9, 131.1, 130.5, 125.3, 125.1, 61.5, 60.8, 54.6, 50.3, 37.9, 37.8, 24.9; IR (KBr pellet) 1651 cm^{-1}; mass spectrum (FAB, glycerol–thioglycerol) 905 (M + H^+). Anal. Calcd for $C_{45}H_{60}N_8O_{12}\cdot 2/3CH_2Cl_2\cdot 4H_2O$ (Found): C, 53.06 (53.25); H, 6.77 (6.91); N, 10.84 (10.41).

BicappedTPTTRENCAM (14) (Scheme I). The crude solid was dissolved in MeOH and precipitated with Et_2O. The flocculent white solid was removed by filtration and dried under vacuum, mp = 262 °C: yield 0.22 g (99%); ^1H NMR (DMSO-d_6) δ 8.8 (br s, 3 H, ArCONH), 8.65 (br s, 3 H, ArCONH), 7.1 (br d, 3 H, ArH), 6.8 (br d, 3 H, ArH), 3.75 (br s, 6 H, RCH_2NHCO), 3.6 (br s, 6 H, RCH_2NHCO), 3.25 (m, 12 H, NCH_2R), 2.05 (br s, 6 H, $NCH_2CH_2CH_2NHCO$); mass spectrum (FAB, glycerol–thioglycerol) 821 (M + H^+); high-resolution mass calcd

Scheme II. Synthetic Route for Mesitylenetriamine

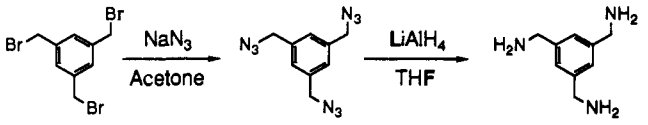

16 17 18

for $C_{39}H_{39}N_8O_{12}$ (found) 821.347 (821.339). Anal. Calcd for $C_{39}H_{48}N_8O_{12}\cdot 2HBr\cdot 2H_2O$ (Found): C, 45.97 (45.61); H, 5.35 (5.04); N, 11.00 (10.80).

Me$_6$bicappedTPTCAM (11) (Scheme I): R_f (30% MeOH/CH_2Cl_2) 0.56. Evaporation of the solvent gave a crystalline solid which was recrystallized from CH_2C_{12}/Et_2O: yield 0.12 g (12%); ^{1}H NMR ($CDCl_3$) δ 8.19 (br t, 6 H, ArCONH), 7.68 (s, 6 H, ArH), 3.65 (s, 9 H, $ArOCH_3$), 3.48 (br m, 12 H, $NCH_2CH_2CH_2NHCO$), 2.57 (br s, 12 H, $NCH_2CH_2CH_2NHCO$), 1.70 (br s, 12 H, $NCH_2CH_2CH_2NHCO$); ^{13}C NMR ($CDCl_3$) δ 163.8, 150.7, 130.3, 125.0, 61.1, 51.6, 38.2, 25.9; IR (KBr pellet) 1654 cm^{-1}; mass spectrum (FAB, glycerol–thioglycerol) 947 ($M + H^+$).

BicappedTPTCAM (15) (Scheme I). The crude solid was taken up in DMF and precipitated with Et_2O. The flocculent white product was filtered on a 0.45 μm nylon filter and dried under vacuum, mp = 260 °C: yield 0.180 g (64%); ^{1}H NMR (DMSO-d_6) δ 8.8 (br s, 6 H, ArCONH), 7.2 (s, 6 H, ArH), 3.8 (m, 12 H, $NCH_2CH_2CH_2NHCO$), 2.95 (br s, 12 H, $NCH_2CH_2CH_2NHCO$), 1.8 (br s, 12 H, $NCH_2CH_2CH_2NHCO$); mass spectrum (FAB, glycerol–thioglycerol) 863 ($M + H^+$); high-resolution mass calcd for $C_{42}H_{55}N_8O_{12}$ (found) 863.394 (863.388). Anal. Calcd for $C_{42}H_{54}N_8O_{12}\cdot 2.25HBR\cdot DMF\cdot 3H_2O$ (Found): C, 46.10 (46.08); H, 5.97 (5.69); N, 10.76 (11.08).

Compounds Prepared via Scheme II.[22] Mesitylenetriazide (17). In a 1-L flask, under an argon atmosphere, compound **16** (10 g, 28 mmol, 1 equiv), NaN_3 (19.68 g, 30.3 mmol, 10.8 equiv), and 350 mL of dry acetone were stirred together and then heated at reflux for 10 h. The reaction mixture was allowed to cool to room temperature and diluted with 250 mL of ether and 250 mL of water. The organic layer was separated and washed with 200 mL of saturated sodium chloride, dried over Na_2SO_4, and concentrated (without heating) under vacuum to give a slightly yellow oil. The pure compound **17** was obtained after chromatography (4.3 × 40 cm gravity column, Davisil 62 60–200 mesh silica, 50% CH_2Cl_2/hexane): R_f(CH_2Cl_2) 0.61; yield 6.60 g (97%). [**Caution**: This step is dangerous; the pure compound should *not* be heated. A blast shield should be used.]

Mesitylenetriamine (18). In a 500-mL flask, under an argon atmosphere, $LiAlH_4$ (3 g, 80.2 mmol, 3 equiv) was suspended in 150 mL of THF. The suspension was cooled in an ice bath, and a solution of compound **17** (6.5 g (26.7 mmol, 1 equiv) in 60 mL of THF) was added dropwise over a period of 1.5 h. After the addition was completed (yellow-pink suspension), the mixture was heated at reflux for 12 h. The mixture was cooled in an ice bath, and 8 mL of water was added slowly. The gray mixture was stirred at room temperature for 20 min and filtered over a pad of Celite. The solvent was removed, and the colorless residue was taken up in 60 mL of CH_2Cl_2, filtered, and concentrated to give a white solid which was dried under vacuum for 12 h: yield 3.88 g (88%); ^{1}H NMR (D_2O) δ 7.22 (q, 3 H, ArH), 3.78 (q, 6 H, $ArCH_2NH_2$). Anal. Calcd for $C_9H_{12}N_3\cdot 0.65H_2O$ (Found): C, 61.09 (61.44); H, 9.28 (9.26); N, 23.74 (23.33).

Compounds Prepared via Scheme III. Dimethyl 2,3-Bis(benzyloxy)terephthalate (19) (Not Shown in Scheme III). Benzyl chloride (24.96 g, 0.197 mmol), KI (29.2 g, 0.176 mmol), and K_2CO_3 (85.8 g, 0.62 mmol) were added to a 2000-mL, round-bottomed flask containing 800 mL of acetone. Following the addition of dimethyl 2,3-dihydroxyterephthalate (20.27 g, 0.09 mmol), the solution was heated to reflux for 96 h. TLC on silica (petroleum ether/ETOAc/MeOH, 15:3:1) showed no starting material (R_f 0.3, streaks to R = 0) and only product dibenzyl ether (R_f 0.87). After cooling to room temperature, the suspension was filtered, and the solids were washed with acetone. The combined filtrates were concentrated, yielding a fine, white, water-soluble precipitate, which was removed by an additional filtration. The filtrate was then evaporated to dryness, and the resulting yellow solid was recrystallized from hot methanol. The yellowish crystals were washed with cold methanol and vacuum dried to give 31.12 g (85%) of the product, mp = 81 °C: ^{1}H NMR ($CDCl_3$) δ 7.6 (s, 2 H), 7.4 (m, 10 H), 5.2 (s, 4 H), 3.9 (s, 6 H); ^{13}C NMR ($CDCl_3$) δ 165.6, 152.6, 136.5, 130.5, 130.15, 128.7, 128.2, 125.5, 76.3, 52.3. Anal. Calcd (Found) for $C_{24}H_{22}O_6$: C, 70.93 (71.02); H, 5.56 (5.48).

2,3-Bis(benzyloxy)terephthalic Acid (20) (Not Shown in Scheme III). Dimethyl 2,3-bis(benzyloxy)terephthalate (11.6 g, 0.029 mmol) was refluxed in a mixture of dimethoxyethane (75 mL) and aqueous sodium hydroxide (150 mL, 3.3 M) for 9 h. Evaporation of the dimethoxyethane followed by the addition of concentrated HCl to the cold (5 °C) aqueous solution caused the precipitation of a white solid which was collected by filtration. The filter cake was washed with water and methanol and vacuum dried (20 μm, 48 g) to give 10.1 g (94%) of the diacid, mp = 188–190 °C: ^{1}H NMR (DMSO-d_6) δ 7.509 (s, 2 H), 7.395 (m, 10 H), 5.049 (s, 4 H). Anal. Calcd (Found) for $C_{22}H_{18}O_6$: C, 69.84 (69.55); H, 4.79 (4.62).

Scheme III. Template Route for Fe(bicappedTRENCAM)

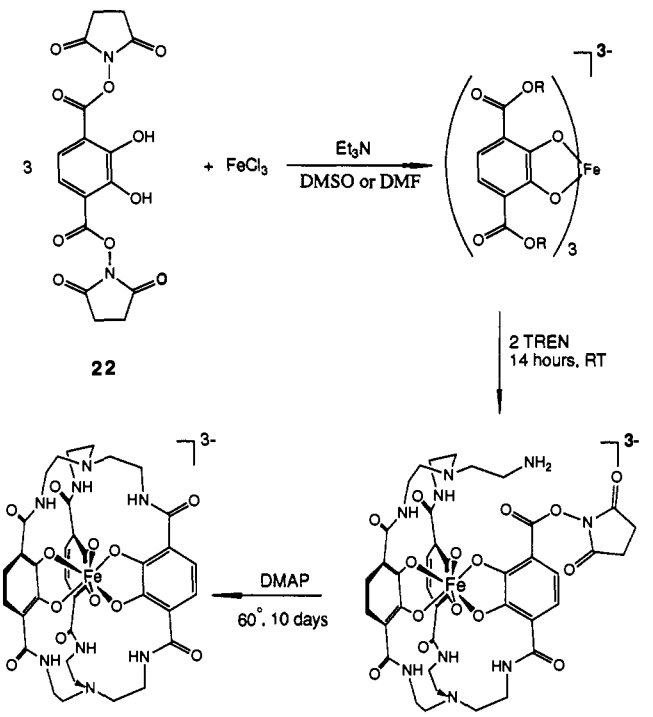

23
[Fe(bicapped TRENCAM)]$^{3-}$

Disuccinimido 2,3-Bis(benzyloxy)terephthalate (21) (Not Shown in Scheme III). In a 500-mL flask, 2,3-bis(benzyloxy)terephthalic acid (6.0 g, 0.016 mmol) and *N*-hydroxysuccinimide (4.02 g, 0.034 mmol) were dissolved in 300 mL of dry dioxane under argon. After cooling to 11 °C in an ice bath, a solution of dicyclohexylcarbodiimide (7.18 g, 0.035 mmol in 100 mL of dioxane) was added dropwise over 1 h. The reaction was warmed to room temperature and stirred 24 h, when TLC showed the absence of starting material at R_f 0. The dicyclohexylurea solids were removed by filtration, and the yellow filtrate evaporated to give an oil from which a white solid precipitated upon the addition of isopropyl alcohol. This solid dissolved upon the addition of more (ca. 200 mL/g) hot isopropyl alcohol. Cooling to room temperature yielded 6.6 g of fluffy white solid (72%), mp = 188–190 °C: ^{1}H NMR ($CDCl_3$) δ 7.8 (s, 2 H), 7.4 (m, 10 H), 5.2 (s, 4 H), 2.8 (s, 8 H); ^{13}C NMR ($CDCl_3$) δ 168.9, 159.8, 154.0, 135.8, 128.6, 128.5, 126.4, 126.3, 76.8, 25.3; IR (KBr, cm^{-1}) 1810 (m), 1775 (m), 1735 (s); mass spectrum (EI) 572 (M^+), 481 ($M - C_7H_7$), 458 ($M - NC_4O_2$). Anal. Calcd (Found) for $C_{30}H_{24}N_2O_{10}$: C, 62.94 (62.72); H, 4.23 (4.17); N, 4.89 (4.91).

Disuccinimido 2,3-Dihydroxyterephthalate (22). Disuccinimido 2,3-bis(benzyloxy)terephthalate (0.5 g, 0.87 mmol) was dissolved in 25 mL of EtOAc. Following the addition of 50 mg of 5% Pd/C catalyst, the reaction was stirred under 1 atm H_2 for 1 h. The suspension of product and catalyst was collected on a Buchner funnel by using Whatman no. 50 paper, and the product subsequently was washed into the desired flask with dimethylformamide by using vacuum filtration. Evaporation of the solvent, followed by vacuum drying, yielded 0.32 g (94%) of a yellow solid: ^{1}H NMR (DMSO-d_6) δ 7.468 (s, 2 H), 2.894 (s, 8 H); ^{13}C NMR (DMSO-d_6) 170.3, 161.0, 150.0, 119.9, 115.7, 25.6.

[Et$_3$NH]$_3$[Fe(bicappedTRENCAM)] by the Template Reaction, 23. A 1-L, three-necked flask was equipped with two addition funnels (A and B), flushed with argon, and charged with 250 mL of DMSO. Disuccinimido 2,3-(dibenzyloxy)terephthalate (2 g, 3.49 mmol) was hydrogenated to give the deprotected disuccinimido 2,3-dihyroxyterephthalate which was washed into a 250-mL, round-bottomed flask with 160 mL of DMSO and kept under an argon atmosphere. Triethylamine

(2.92 ml, 21 mmol) was added followed immediately by a DMSO solution of anhydrous ferric chloride (0.188 g, 1.2 mmol in 60 mL of DMSO). The resulting dark brown solution was transferred via cannula to addition funnel A, and DMSO was added to make a total volume of 250 mL. To addition funnel B was added a solution of TREN (0.333 g, 2.32 mmol) in 250 mL of DMSO. The solutions in the two addition funnels were added simultaneously to the stirring DMSO over a period of 1.5 h. The reaction was stirred at room temperature for 14 h before adding 4-(dimethylamino)pyridine (DMAP, 0.6 g, 4.9 mmol) and heating the reaction to 60 °C.

The progress of the reaction was monitored by analytical HPLC, by using a Hamilton PRPI column (4.6 × 250 mm), a flow rate of 1.5 mL/min, and an ion-pairing solvent system (A = 0.01 M Et_3NH/HCO_2H, pH 10.2, B = 0.01 M Et_3NH/HCO_2H), and a Hewlett-Packard diode array detector (254 or 450 nm). By using a gradient of 10–50% B (5%/min) followed by 50–100% B (10%/min), the ferric monoactive ester intermediate eluted at 10.4 min, and the product Fe(bicappedTRENCAM) eluted at 7.8 min. The reaction was judged complete when no more ferric monoactive ester intermediate was detected (10 days).

The crude ferric complex was isolated from DMSO by first vacuum distilling off the DMSO to concentrate the solution to ca. 20 mL. Following the addition of 2 mL of 1 M NaOH, the ferric complexes were precipitated by addition of 50 mL of acetone and 50 mL of diethyl ether. The brick red solid was collected by filtration (medium frit) and washed with acetone. Any remaining soluble ferric complexes were isolated by concentrating the filtrate to DMSO and repeating the precipitation scheme by using a larger proportion of diethyl ether.

The combined solids were dissolved in 250 mL of HPLC solvent A (0.01 M Et_3N/HCO_2H in H_2O) while maintaining the pH at 10.2 by addition of 1 M NaOH. The solution was then applied to a preparative Hamilton PRPI HPLC column (2.5 × 22.5 cm) in 40 6.25-mL batches. By using the same solvent system described above, Fe(bicappedTRENCAM) eluted at 7.9 min (detector at 451 nm). Fractionation of the peak (0.5 min/fraction) gave three fractions of pure product and two which were concentrated and later reinjected.

The combined fractions of pure Fe(bicappedTRENCAM) were concentrated to 20 mL. The pH was lowered to 4.5, and the resulting dark brown precipitate was collected on a fine frit and washed with H_2O (10 mL) and CH_3OH (10 mL). The solid, suspended in 10 mL of H_2O, dissolved to form the soluble red trianion upon the addition of 200 μL of Et_3N. Evaporation to dryness once from H_2O and twice from CH_3OH, followed by vacuum drying (40 μm, 48 h), gave 0.62 g (48%) of $[Et_3NH]_3$[Fe(bicappedTRENCAM)], mp > 360 °C; mass spectrum (FAB, negative ion) 830 ($[M + 2H^+]^-$). Anal. Calcd (Found) for $FeC_{54}H_{84}N_{11}O_{12}\cdot 3H_2O$: C, 54.53 (54.73); H, 7.62 (7.31); N, 12.96 (12.98); Fe, 4.70 (4.72).

Na_3[Fe(bicappedTRENCAM)] (24). $(Et_3NH)_3$[Fe(bicappedTRENCAM)]·$3H_2O$ (180 mg, 0.15 mmol) was dissolved in 10 mL of H_2O, applied to a cation exchange column (AG50W-X8, Na^+ form, 4 × 32 cm), and eluted with H_2O. Evaporation of the red fraction followed by vacuum drying gave Na_3[Fe(bicappedTRENCAM)]: mass spectrum (FAB, negative ion) 830 ($[M + 2H^+]^-$), 852 ($[M + H^+ + Na]^-$), 874 ($[M + 2Na^+]^-$); IR (KBr, cm^{-1}) 3400 (s), 3190 (m), 2956 (w), 2882 (w), 1605 (s), 1553 (s), 1448 (m), 1343 (m), 1237 (m), 1202 (s), 744 (m), 657 (m), 570 (w).

BicappedTRENCAM (25). $[Et_3NH]_3$[Fe(bicappedTRENCAM)]·$3H_2O$ (70 mg, 59 μmol) was dissolved in 3.0 mL of H_2O. Glacial acetic acid (1.5 mL) was added, causing the formation of a blue/brown solution to which was added $Na_2CaEDTA$ (244 mg). After stirring for 45 min, a colorless precipitate was removed by filtration, and the clear yellow filtrate was applied to a reverse-phase HPLC column (21.4 × 250 mm, 8 μm Dynamax C-18) in 3-mL batches and eluted with 0.01 M AcOH (A = H_2O, B = CH_3OH) by using a gradient of 10–100%B (10%/min, flow rate 15 mL/min, 340 nm). Demetalated bicappedTRENCAM eluted at 8 min. Evaporation of the solvent gave a slurry from which a light yellow solid precipitated upon the addition of hot CH_3OH. After vacuum drying, 41 mg (89%) of a slightly off-white powder was obtained, mp = 332 °C dec: ^1H NMR (D_2O, pH 12) δ 6.61 (s, 6 H), 3.39 (br s, 12 H), 3.30 (s, MeOH), 2.71 (br s, 12 H); mass spectrum (FAB, positive ion) 779 ($[M + H^+]^+$); IR (KBr, cm^{-1}) 3376 (s), 3307 (m), 2805 (s), 2743 (w), 1646 (s), 1603 (s), 1550 (s), 1485 (m), 1428 (s), 1335 (s), 1247 (m), 1230 (m), 1190 (m), 1170 (m), 1034 (m), 867 (m), 833 (m), 821 (w), 796 (m), 753 (w), 730 (m), 641 (m). Anal. Calcd (Found) for $C_{36}H_{42}N_8O_{12}\cdot{}^1/_2CH_3OH\cdot{}^1/_2H_2O$: C, 54.53 (54.65); H, 5.65 (5.64); N, 13.94 (13.81).

Electrochemistry. Voltammograms were measured by using a Princeton Applied Research Potentiostat/Galvanostat (model 173) and a Princeton Applied Research Universal Programmer (Model 175). Pulse polarograms were measured by using a Princeton Applied Research Polarographic Analyzer (Model 174A) and recorded on a Houston Omnigraphics 2000 X-Y recorder. Dropping mercury was used as the working electrode, a Pt wire as the counter electrode, and a saturated calomel electrode (SCE) as the reference electrode in a one-compartment cell. The SCE reference used has a potential of +0.22 V vs NHE as calculated by measuring the formal reduction potential of the $Fe(CN)_6^{3-/4-}$ couple in 1 M H_2SO_4 at glassy carbon. The pH was measured with a Brinkmann Instruments Metrohm pH-102 meter and a calomel combination electrode.

The supporting electrolyte was 0.4 M $NaClO_4$, and the buffer was 50 mM Na_2HPO_4, adjusted to the desired pH with ca. 0.45 M NaOH or HCl. Prior to the addition of analyte, the buffer/electrolyte (background) solution was deoxygenated for at least 1.0 h with a stream of Ar (deoxygenated by pretreatment through a $V^{II}/Zn(Hg)$ solution) that was used throughout the experiment. Between 0.4 and 1.0 mmol of ligand were added to the deoxygenated background solution (pH > 11) followed by the addition of an equivalent or slight excess amount of Fe^{3+} (stock solution was 50.29 (8) mM Fe^{3+} in 0.1000 (2) M HCl) solution delivered by using a calibrated Gilmont pipet, which addition turned the clear solution to a red wine color. The solution was mixed until all the ligand dissolved, and then, after allowing the excess Fe^{3+} to precipitate (ca. 30 min), the solution was filtered through a 0.2-μm Gelman Acrodisc. The $E^{\circ\prime}$ and the number of electrons being transferred (n) were measured by DPP and NPP at several pH values between 6 and 12. The pH dependent electrochemical studies for each complex were performed at three or more temperatures (Lauda 2-K/R temperature bath, ±1 °C), except for Fe(bicappedTRENCAM) which was studied at only two temperatures. In order to conserve ligand in the electrochemical studies, the same solution, kept continuously under Ar, was used in consecutive experiments. This resulted in a dilution of ca. 50% from the initial to the final solution concentration.

Solution Thermodynamic Studies. Water was deionized, distilled, and further purified by a Millipore cartridge system (resistivity = 18 × 10^6 ohms-cm). The water was then degassed and put under an inert atmosphere.

Spectrophotometric data sets were collected on a custom-built automatic titration apparatus composed of an HP 8450 UV–vis spectrophotometer, a Fisher Accumet pH meter with a calomel combination electrode, a Metrohm 655 Dosimat automatic buret, a water-jacketed 10-cm quartz cell, a Brinkmann Lauda K-2/R constant temperature bath, and a computer equivalent to an IBM-XT. Ligand titrations were performed with approximately 10 μm ligand and ferric complex titrations with approximately 20 μm ferric complex. The BASIC program TIMBERWOLF was used to run the apparatus.[23] Data analysis was performed on an IBM-AT computer with the REFSPEC[24] spectral componentization and least-squares program. The compounds were added to high pH aqueous solutions at 0.1 M ionic strength (KCl (ferric complex studies) or $(CH_3CH_2CH_2)_4NCl$ (ligand studies)) held at 25 °C. The solution was titrated to low pH with 0.1 M HCl. After the titration, the solution was again raised in pH with concentrated KOH to check for hysteresis (i.e., irreversible behavior); none was found. All experiments were run under an argon atmosphere, excluding O_2. The electrode was calibrated in concentration units with degassed solutions of $10^{-2.30}$ M HCl and $10^{-2.295}$ M KOH at 0.1 M ionic strength (KCl). The appropriate value of $10^{-13.78}$ for K_w was used.[25]

NMR titration data were collected on custom-built 180- and 200-MHz FT spectrometers. BicappedTRENCAM was approximately 27 mM (5 mm tube) or approximately 5 mM (10 mm tube). Deuterium oxide was degassed and put under an inert atmosphere. The hydrogen ion electrode was calibrated in concentration units ($p[H^+] = -\log [H^+]$) as described above, and the correct value of p[D] was calculated by using the relationship $p[D] = p[H] + 0.040$.[26] The pD was adjusted with degassed solutions of CsOD and DCl at an ionic strength of 0.1 M (CsCl). Data analysis was performed on an IBM-AT computer by using the MARQFIT nonlinear least-squares program.[27]

(21) Macrobicycles were precipitated out of DMF or MeOH by Et_2O. Where more than one solvent was tried, only the most effective is listed in the experimental although the other may appear in the elemental analysis as prepared from other runs. The solvents DMF and MeOH as well as excess HBr proved extremely difficult to remove and remained after months of continuous vacuum at 20 μm Hg.

(22) Heyer, D.; Lehn, J.-M. *Tetrahedron Lett.* **1986**, *27*, 5869.

(23) Loomis, L. D. Ph.D. Dissertation, University of California at Berkeley, 1986.

(24) Turowski, P. N.; Rodgers, S. J.; Scarrow, R. C.; Raymond, K. N. *Inorg. Chem.* **1988**, *27*, 474.

(25) Martell, A. E.; Smith, R. M. *Critical Stability Constants*; Plenum: New York, 1976; Vol. IV, p 1.

(26) Bates, R. G. *Determination of pH, Theory and Practice*; John Wiley & Sons: New York, 1964.

(27) Schreiner, W.; Kramer, M.; Krischer, S.; Langsam, Y. *PC Tech Journal* **1985**, 170.

Table I. Crystal and Data Collection Details for Fe(bicappedTRENCAM)

Crystal Parameters[a]	
formula	$C_{36}H_{36}N_8O_{12}FeNa_3 \cdot 17.5H_2O$
space group	$P6_3/m$ (no. 176)
a, Å	13.785 (3)
c, Å	16.244 (5)
V, Å^3	2673 (2)
formula wt, amu	1212.8
z	2
d_c, g/cm^3	1.51
d_o, g/cm^3	1.45
μc, cm^{-1}	3.97
size of crystal, mm	0.13, 0.13, 0.44
Data Collection Details	
radiation, λ, Å	Mo Kα, 0.71073[b]
monochromator	highly oriented graphite ($2\theta_m$ = 12.2°)
2θ range, °	$3 \le 2\theta \le 55$
reflcns measd	$0 \le h \le 14$ $0 \le k \le 15$ $-21 \le l \le 21$
scan type	θ–2θ
scan speed, θ, deg/min	min. 1.1, max 6.7
scan width, $\Delta\theta$, deg	variable, 0.6 + 0.35[tan (θ)]
background	measd over 0.25 ($\Delta\theta$), added to each end of scan
aperture, mm	to crystal, 173 vertically, 3.0 horizontally variable, 2.0 + 1.0[tan (θ)]
total data collected	4828
no. of unique data, R_{av}, %	2120, 2.4
no. of obsd data $(F_o^2) \ge 3\sigma(F_o^2)$	1069
Refinement Parameters	
R, %	4.38
R_w, %	5.16
R_{all}, %	18.78
p factor	0.04
GOF	1.62
no. of variables	158

[a] Estimated standard deviations of the last significant digit are given in parentheses in this and all subsequent tables. [b] See footnote 28.

Competition experiments were performed on an HP 8450 spectrometer by using 10:1 CDTA/Fe(bicappedTRENCAM) and a 1-cm cell. The solutions were approximately 100 μm in Fe(bicappedTRENCAM). Ionic strength was 0.1 M (Et_4NCl). The pH was adjusted with Et_4NOH and HCl. The electrode was calibrated in concentration units as described above. The pH was buffered by the excess CDTA at several different pH's from pH 5.1–6.8.

Structural Studies. Deep red crystals of Na_3[Fe(bicappedTRENCAM)]·nH$_2$O were obtained from an aqueous methanol solution. The data cryatal (Table I) was mounted in a thin-walled glass capillary and examined by Laue and precession photographs. Intensity data were collected on a Enraf-Nonius CAD-4 diffractometer.[28] Final cell parameters were obtained by least-squares refinement of the angular settings of 24 reflections well-separated throughout reciprocal space in the 2θ range $20° \le 2\theta \le 27°$. Crystal and data collection details are shown in Table I.

Inspection of the list of F_o's showed that $F_{hkl} \neq F_{khl}$, ruling out all space groups derived from the Laue group $P6/mmm$. Systematically absent reflections ($00l$, $l = 2n + 1$) were consistent with a 6_3 axis parallel to c. Thus the only possible space groups in the Laue group $P6/m$ were $P6_3$ (no. 173) and $P6_3/m$ (no. 176). Although the structure was solved

(28) Data were collected by applying θ–2θ scan techniques (scan speed variable min. 1.1, max 6.7°/min) with Mo Kα radiation (λ = 0.71073 Å) at 20 °C in the 2θ range $3° \le 2\theta \le 55°$ ($0 \le h \le 14$, $0 < k < 15$, $-21 < l \le 21$). The intensities of three standard reflections [(−3,−3,4), (−5,5,−5), and (−6,9,0)] were remeasured every 2 h of X-ray exposure time. Three orientation check reflections were remeasured after each 200 intensity measurements. A new orientation matrix was calculated from an array of 24 reflections if any of the orientation standards was offset from its predicted position by more than 0.1°. Reorientation was necessary once during data collection. Azimuthal scans were recorded at the end of the data collection for five reflections near χ = 90° at 10° increments of rotation of the crystal about the diffraction vector. Total data collected = 4828 reflections. The raw intensity data were converted into structure factor amplitudes (and their esd's) by correcting for scan speed, background, and Lorentz and polarization effects. Inspection of the list of intensity standards revealed that no correction for decay was necessary (change <1% over the 62 h of X-ray exposure time). The azimuthal scan data showed a variation of 1.4% for the average curve, and no absorption correction was applied.

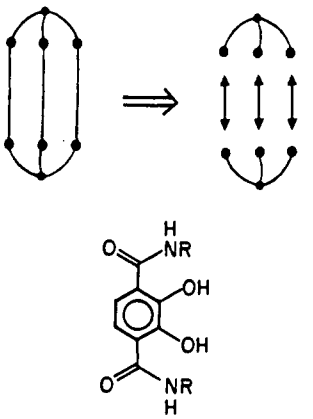

Figure 1. Retrosynthetic scheme for the preparation of macrobicyclic ligands incorporating symmetrical bidentate and bifunctional ligand units. Here the double-headed arrows represent the 2,3-dihydroxyterephthalamide binding subunit.

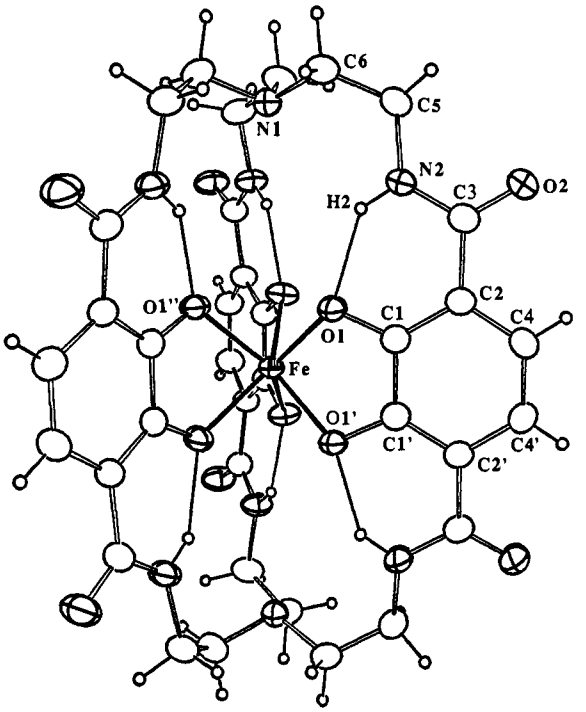

Figure 2. An ORTEP drawing of the Fe(bicappedTRENCAM) anion viewed with the 3-fold axis vertical. The thermal ellipsoids are scaled to represent the 50% probability surface. Hydrogen atoms are given arbitrarily small spheres for clarity.

Table II. Occupancy Factors for the Disordered Water Oxygen Atoms in the Fe(bicappedTRENCAM) Structure

oxygen atom[a]	Wyckoff position	site occupation factor	H_2O per unit cell
0101	i	1.0[b]	12.0
0102	i	0.55	6.6
0103	i	0.45	5.4
0104	h	0.25	3.0
0105	i	0.605	7.260
0106	h	0.056	0.672
0107	h	0.132	1.548
0108	i	0.213	2.556
0109	h	0.076	0.912

[a] Atoms 0101–0109 represent an electron density equivalent to 40 oxygen atoms per unit cell. [b] The site occupancy factors of 0101–0104 were fixed in the final least-squres cycles, while those for 0105–0109 were refined.

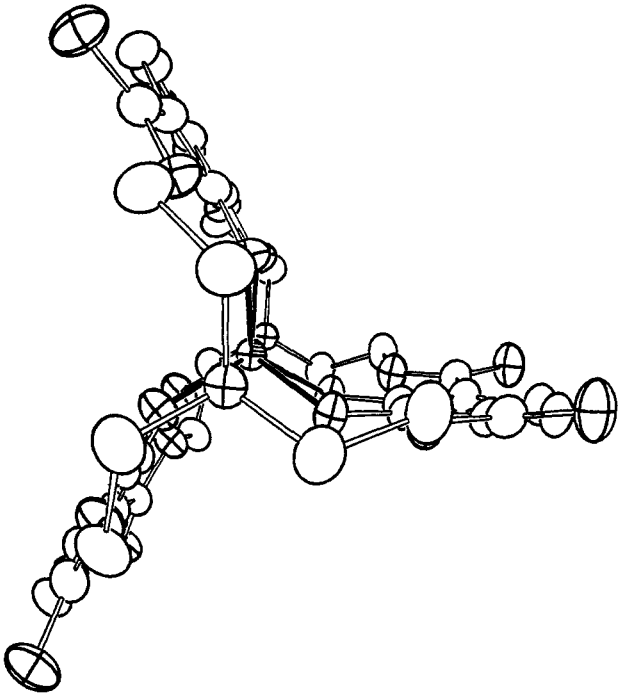

Figure 3. An ORTEP diagram of the Fe(bicappedTRENCAM) anion viewed down the 3-fold axis.

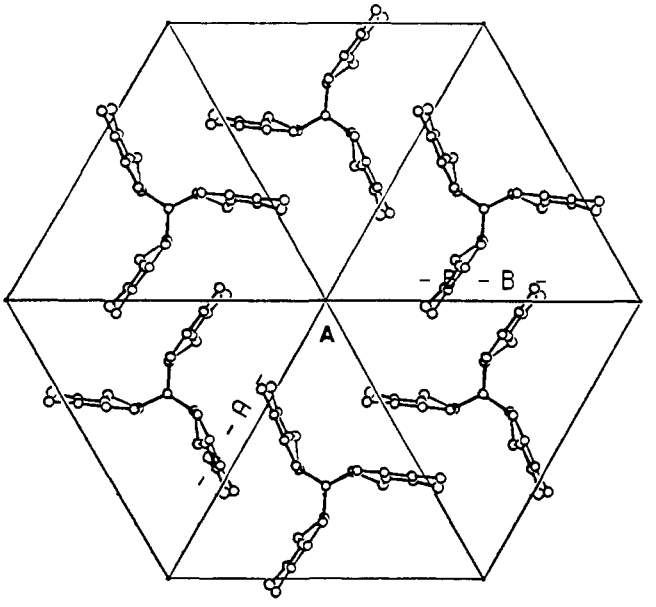

Figure 4. An ORTEP drawing with a view of three unit cells of Fe(bicappedTRENCAM) showing the full hexagonal packing array. These triskelion anions are in the upper half of the cell and the other three below. The disordered sodium–water lattice resides at position A.

in $P6_3$ by use of direct methods (MULTAN/82),[29] subsequent analysis showed the correct space group to be $P6_3/m$.

The iron atom lies at the intersection of the 3-fold axis with the mirror plane (Wyckoff position c, site symmetry $\bar{6}$) such that the iron atom is coordinated by six catechoyl amide oxygen atoms in a trigonal prismatic geometry. The two tertiary amine nitrogen atoms (N1,N1′) lie on the same 3-fold axis as the iron atom. The Fe(bicappedTRENCAM) anion with crystallographic numbering scheme is depicted in Figure 2. A view down the 3-fold axis is presented in Figure 3.

One sodium cation (Na1) per trianion was found in a difference Fourier map (Wyckoff position b, site symmetry $\bar{3}$). It is coordinated by one disordered water molecule per asymmetric unit in a general position (O102, site occupancy factor 0.55; O103, site occupancy factor 0.45—see Table II) giving a distorted octahedral coordination geometry about Na1.

Microprobe analysis of single crystals gave a result of $(Na/Fe)_{av}$ = 3.1 (4), ensuring that the compound must be Na_3[Fe(bicappedTRENCAM)]·$n$$H_2O$ and not the protonated salt Na[Fe(H_2bicappedTRENCAM)]·$n$$H_2O$. Since only one of the three sodium cations was found and because the remaining peaks in the difference Fourier had intensities less than 3e⁻/Å³, it was assumed that the remaining electron density represented disordered water positions and the four missing sodium cations per unit cell. None of the peaks could be assigned a specific sodium position, so the electron density in this disordered sodium–water lattice was modelled as partially occupied water oxygen positions. Site occupancies are given in Table II. The disordered sodium–water portion of the structure resides at position A in Figure 4.

Atoms O101–O109 represent a scattering power of 40 oxygen atoms (320 e⁻) per unit cell. The scattering power of $4Na^+$ (40 e⁻) was subtracted from the 320 e⁻ total scattering power of the sodium–water lattice, and the result was divided by 8 (8e⁻ per water oxygen atom) yielding the formula Na_3[Fe(bicappedTRENCAM)]·17.5H_2O. The observed density gives a molecular weight consistent with the formulation Na_3[Fe(bicappedTRENCAM)·15H_2O ± 1.3H_2O. This value is within 2σ of the value calculated by the X-ray structure. Since the material is

(29) Main, P.; Fiske, S. J.; Hull, S. E.; Lessinger, L.; Declercq, J.-P.; Woolfson, M. M. MULTAN/82 *System of Computer Programs*; University of York: York, 1982.

Table III. Selected Bond Distances for Fe(bicappedTRENCAM)[a]

	Anion		
Fe–O1	2.012 (2)	C5–C6	1.522 (4)
C1–O1	1.333 (3)	C6–N1	1.474 (3)
C1–C1′	1.437 (5)	N2–H2	0.89 (4)
C1–C2	1.390 (4)	C4–H4	0.90 (4)
C2–C3	1.478 (4)	C5–H5A	1.01 (4)
C2–C4	1.413 (4)	C5–H5B	0.99 (4)
C4–C4′	1.364 (6)	C6–H6A	1.05 (4)
C3–O2	1.259 (3)	C6–H6B	1.00 (4)
C3–N2	1.332 (4)	H2–O1	1.89 (4)
N2–C5	1.463 (4)		
	Cation		
Na1–O102[b]	2.511 (6)	Na1–O103	2.415 (7)
	Nonbinding Distances		
O1–O1′[b]	2.526 (4)	O2–O101[c]	2.798 (3)
O1–O1″	2.713 (3)	N2–O1	2.620 (3)

[a] Primed atoms represent transformed coordinates of the type x, y, $^1/_2 - z$. [b] O102 and O103 are the disordered water positions around Na1 (Table S3, Figures 2 and 5). [c] O101 is likely hydrogen bonded to O2 however no water hydrogen atoms could be identified in the difference Fourier maps and none of the water hydrogen atoms was added to the structure model (see Figure 3).

Table IV. Selected Bond Angles for Fe(bicappedTRENCAM)[a,b]

	Anion		
O1–Fe–O1′	77.75 (11)	C3–N2–C5	122.7 (3)
O1–Fe–O1″	84.78 (8)	C3–N2–H2	119 (3)
O1–Fe–O1‴	134.18 (4)	C5–N2–H2	118 (3)
Fe–O1–C1	111.2 (2)	N2–C5–C6	111.4 (3)
O1–C1–C2	125.4 (2)	N2–C5–H5A	109 (2)
O1–C1–C1′	114.11 (14)	N2–C5–H5B	110 (2)
C1′–C1–C2	120.4 (2)	C6–C5–H5A	109 (2)
C1–C2–C3	121.7 (2)	C6–C5–H5B	104 (2)
C1–C2–C4	117.9 (3)	H5A–C5–H5B	114 (3)
C3–C2–C4	120.3 (3)	C5–C6–N1	115.9 (3)
C2–C3–N2	117.6 (3)	C5–C6–H6A	114 (2)
C2–C3–O2	120.8 (3)	C5–C6–H6B	114 (2)
O2–C3–N2	121.5 (3)	N1–C6–H6A	108 (2)
C2–C4–C4′	121.6 (2)	N1–C6–H6B	101 (2)
C2–C4–H4	117 (3)	H6A–C6–H6B	103 (3)
C4′–C4–H4	121 (3)	C6–N1–C6″	108.8 (2)
		N2–H2–O1	138 (4)
	Cation		
O102–Na1–O102*	180.0	O103–Na1–O103*	18.0
O102–Na1′–O102**	105.3 (2)	O103–Na1–O103**	79.7 (3)
O102–Na1–O102***	74.7 (2)	O103–Na1–O103***	100.3 (3)

[a] Primed atoms represent transformed coordinates of the type: (′) x, y, $^1/_2 - z$; (″) $1 - y$, $x - y$, z; (‴) $1 - y$, $x - y$, $^1/_2 - z$ (see Figure 1). [b] Starred atoms represent transformed coordinates of the type: (*) $-x$, $-y$, $-z$; (**) $-y$, $-(y - x)$, z; (***) y, $y - x$, $-z$ (see Figure 2).

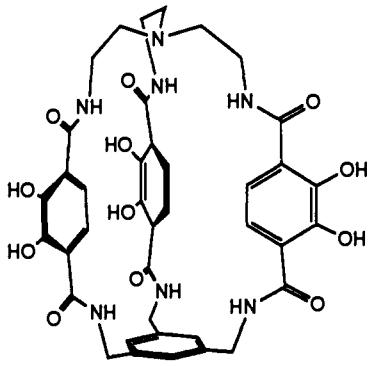

Bicapped TRENMECAM
12

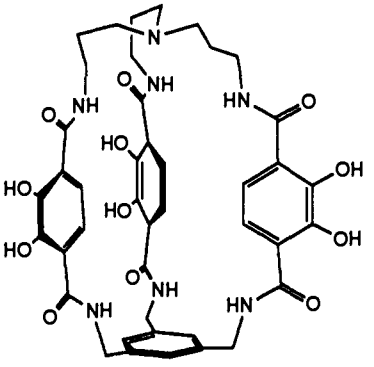

Bicapped TPTMECAM
13

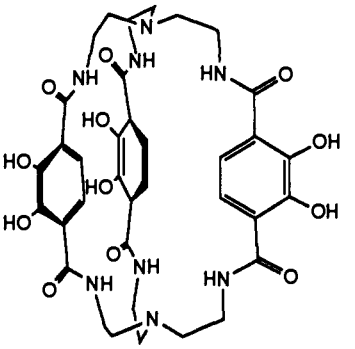

Bicapped TRENCAM
25

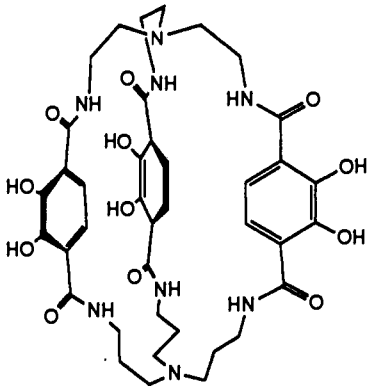

Bicapped TPTTRENCAM
14

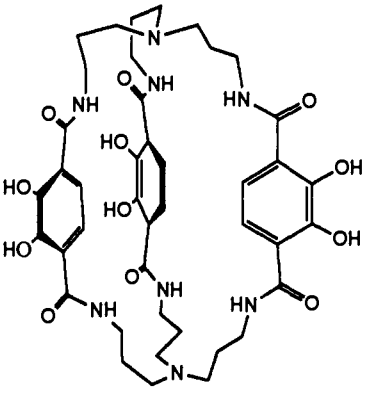

Bicapped TPTCAM
15

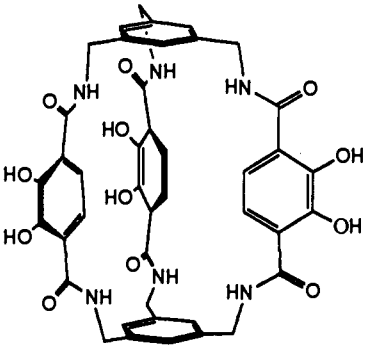

Bicapped MECAM
26

Figure 5. Macrobicyclic iron(III) sequestering agents discussed in this manuscript, their abbreviated names and numeric symbols used herein.

hygroscopic and because the X-ray data are more sensitive to the water stoichiometry, the formulation with $17.5H_2O$ was taken to be correct.

Full-matrix least-squares refinements were employed by using the 1069 independent reflections with $F_o^2 > 3\sigma(F_o^2)$. Atomic scattering factors were taken from the *International Tables for X-ray Crystallography*.[30] Refinement of 158 variables, including positional and anisotropic thermal parameters, gave $R = 4.38\%$, $R_w = 5.16\%$, and GOF = 1.62.[31] Bond distances are listed in Table III and bond angles in Table IV.[32]

Results and Discussion

Synthesis. Two synthetic approaches have been used in the synthesis of the macrobicycles reported here. The first, shown in Scheme I, is a traditional synthetic organic, high-dilution route.[10,33] The key step in this route (Scheme I) is the coupling of two tripodal moieties via a triple amide bond forming reaction. This was performed in THF in the presence of triethylamine under high dilution conditions and afforded the methyl-protected compounds **8**, **9**, **10**, and **11** in 10–13% yields. The tripods **5** and **7** used in this step were made from the known compound **1** in three steps in 78–83% overall yield. Deprotection afforded the macrobicyclic ligands **12**, **13**, **14**, and **15** in 52–99% yield by reaction with BBr_3 in $CHCl_3$. Five ligands have been synthesized by this route to date (Figure 5).

The second synthetic method used is shown in Scheme III and is by far the most efficient route. This conceptually simple approach circumvents the high-dilution reaction by use of a transition metal as a template.[34,35] Elegant examples of the use of metal ions as templates can be found in the synthesis of macrobicyclic cobalt amine sepulchrate complexes by Sargeson and co-workers[36] and in the preparation of catenands by Dietrich-Buchecker, Sauvage, and Kern.[37] Here we have organized three difunctionalized catechols about a ferric ion, enabling the macrobicyclic complex **25** to be formed by reaction with 2 equiv of TREN. At the time this research was initiated, however, a half-cage template route capable of making macrobicycles with different capping groups was not satisfactorily worked out. Since a thorough investigation of how the bicyclic structure affects the stability and chemistry of Fe(III) complexation requires a series of compounds in which the ligand's cavity size, flexibility, and charge are varied, the high-dilution route was used to synthesize the compounds **12**, **13**, **14**, and **15**.

Structural Studies. The structure reported here is the first for any hexadentate catechol analogue of enterobactin. In this case

(30) Cromer, D. T.; Waber, J. T. *International Tables for X-ray Crystallography*; Kynoch: Birmingham, 1974; Vol. IV, Tables 2.2B and 2.3.1.
(31) GOF, goodness-of-fit = $[\sum w(|F_o| - |F_c|)^2/(N_{obs} - N_{var})]^{1/2}$ where F is the dependent variable; $R = \{\sum(|F_o| - |F_c|)^2/\sum F_o^2\}^{1/2}$; $R_w = [\sum w(|F_o| - |F_c|)^2/\sum wF_o^2\}^{1/2}$; $w = 4F_o^2/\sigma^2(F_o)^2$ and $\sigma^2(F_o)^2 = \sigma_o^2(F_o^2) + (pF^2)^2$.
(32) Structure factor listings and other material appear in the supplementary material.
(33) Ziegler, K.; Eberle, H.; Ohlinger, H. *Liebigs Ann. Chem.* **1933**, *504*, 94.
(34) Thompson, M. C.; Busch, D. J. *J. Am. Chem. Soc.* **1964**, *86*, 3651.
(35) Melson, G. A. *Coordination Chemistry of Macrocyclic Compounds*; Plenum: New York, 1979.
(36) Geue, R. J.; McCarthy, M. G.; Sargeson, A. M. *J. Am. Chem. Soc.* **1984**, *106*, 8282.
(37) Dietrich-Buchecker, C. O.; Sauvage, J.-P.; Kern, J. M. *J. Am. Chem. Soc.* **1984**, *106*, 3043. Dietrich-Buchecker, C. O.; Kern, J. M.; Sauvage, J.-P. *J. Chem. Soc., Chem. Commun.* **1985**, 760.

the coordination geometry around the metal center is, remarkably, trigonal prismatic (Figure 2). The iron atom resides on a special position with C_{3h} symmetry in the center of the crystallographically required trigonal prism made by the six catechol oxygen atoms. The trigonal prism is slightly compressed along the 3-fold axis. The oxygen–oxygen separation for mirror related atoms is shorter than that for atoms related by the 3-fold axis (O1–O1′ = 2.526 (4) Å; O1–O1″ = 2.713 (3) Å). Trigonal prismatic coordination is a geometry previously unknown for Fe(III) although geometries intermediate[38,39] between octahedral and trigonal prismatic have been observed for ferric complexes of bidentate ligands with relatively small bite differences.[40–42] Although disfavored by ligand–ligand repulsion, there is no ligand field barrier to a trigonal prismatic coordination in a high-spin d^5 complex.[39]

As shown in Figure 2, the entire catechoyl amide group is planar due to the trans configuration of the amide and a strong hydrogen bond between the amide proton and the coordinated catechol oxygen. The result is a highly stable ligand structure which incorporates three planar catechoyl amide groups and six strong amide hydrogen bonds. This imposes the trigonal prismatic geometry on the metal. To accommodate this ligand geometry, the metal lies 0.81 Å out of the catechol plane, giving a 30.79 (12)° dihedral angle between this plane and the plane defined by the iron and the two ligating oxygen atoms forming the prochiral triskelion shown in Figure 3. No crystal structure analysis of ferric enterobactin or an analogue is yet available. A geometry for the amide bonds and complex conformation was predicted by Llinas et al. based on an NMR study of enterobactin and its gallium complex, and these authors ruled out strong amide–catechol oxygen hydrogen bonding in the metal complex.[43] This has been predicted to be important by Shanzer et al., although not predicted for ligand and metal conformations from energy minimization calculations.[44] As seen in the side view of the complex (Figure 2) both tertiary amines are in the "in" conformation.[45] The bite angle in this structure of 77.75 (11)° is the smallest yet seen for a ferric catecholate.[38] It is unclear, however, if this is the "natural" bite angle for the 2,3-dihydroxyterephthalamide binding subunit or if it results from the novel trigonal prismatic structure found here. A complete list of bond distances and angles is given in Tables III and IV.[46]

That the ferric complex has assumed this unusual trigonal prismatic geometry as its lowest energy conformation leads to two important thermodynamic conclusions. The first is that preorganization of the ligand for metal binding is disfavored (vide infra). Secondly, the trigonal prismatic coordination could be considered a relatively high-energy product, in comparison to a molecule with octahedral geometry. Both of these would serve to decrease the observed formation constant. The net effect of these results, as will be shown below, is a dominance of the iron binding equilibria by the enthalpic driving force of the binding subunits.

Solution Thermodynamics. Ligand Studies. The bicapped-TRENCAM ligand **25** was studied by the spectrophotometric method from pH 11 to pH 2. In the family of spectra generated

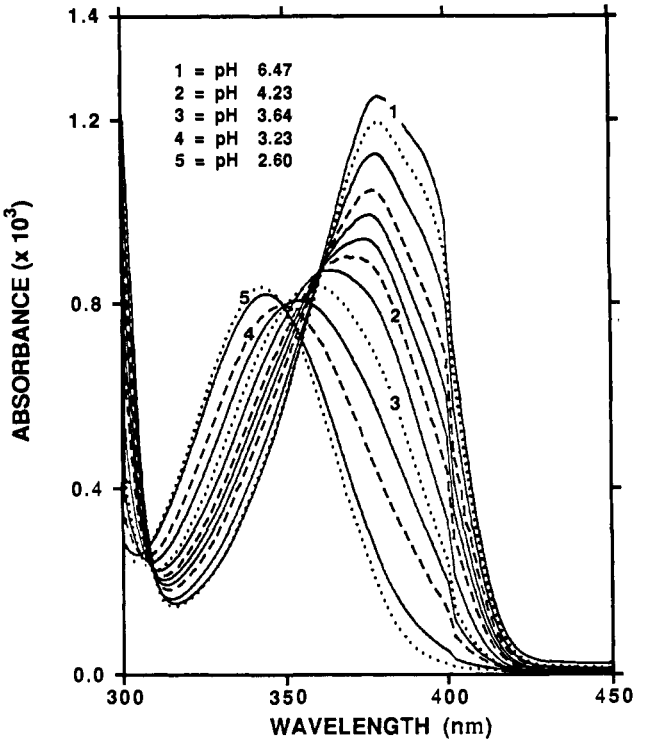

Figure 6. Family of spectra generated by titration of the bicapped-TRENCAM ligand from pH 6.5 to 2.6. The concentration of ligand is approximately 10 μM at a constant ionic strength of 0.1 M (Et_4NCl).

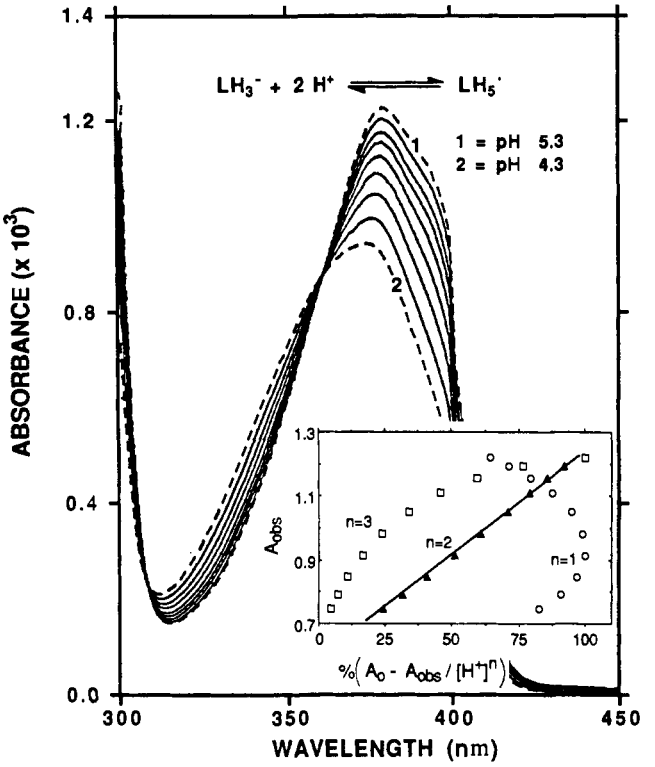

Figure 7. Isosbestic region generated by titration of the bicapped-TRENCAM ligand. [Inset is a plot of A_{obs} versus $(A_o - A_{obs})/[H^+]^n$ which is linear only for $n = 2$. The slope gives an estimate of the log equilibrium constant = 8.7.]

(Figure 6), two buffer regions were found, one from pH 7.6 to pH 3.8, and another from pH 3.8 to below pH 2.8. Both of the buffer regions demonstrate isosbestic behavior, indicating the presence of only two absorbing species in solution for each buffer region—giving three species in total. The raw data for the first buffer region were analyzed by means of a Schwarzenbach plot[47]

(38) Wentworth, R. A. D. *Coord. Chem. Rev.* **1972**, *9*, 171.
(39) Larsen, E.; LaMar, G. N.; Wagner, B. E.; Parks, J. E.; Holm, R. H. *Inorg. Chem.* **1972**, *11*, 2652.
(40) Raymond, K. N.; Isied, S. S.; Brown, L. D.; Fronczek, F. R.; Nibert, J. H. *J. Am. Chem. Soc.* **1976**, *98*, 1767.
(41) Hoskins, B. F.; Kelley, B. P. *J. Chem. Soc., Chem. Commun.* **1968**, 1517.
(42) Wieghardt, K.; Bossek, U.; Chauder, P.; Herrmann, W.; Menke, B. C.; Weiss, J. *Inorg. Chem.* **1982**, *21*, 4308.
(43) Llinas, M.; Wilson, D. M.; Neilands, J. B. *Biochemistry* **1973**, *12*, 3836.
(44) Shanzer, A.; Libman, J.; Lifson, S.; Felder, C. E. *J. Am. Chem. Soc.* **1986**, *108*, 7609.
(45) Simmons, H. E.; Park. C. H. *J. Am. Chem. Soc.* **1968**, *90*, 2428. Park. C. H.; Simmons, H. E. *J. Am. Chem. Soc.* **1968**, *90*, 2429.
(46) There are six water molecules close to the anion (one per asymmetric unit, O101), which are probably hydrogen bonded to O2. The identified sodium cation per anion resides on a special position with 3-fold symmetry. It is coordinated by a disordered water molecule (O102, O103) in a disorted octahedral fashion at Na–O distances of 2.551 (6) and 2.415 Å (located at position A in Figure 4). Distances and angles in the disordered sodium water lattice cannot be assigned due to the disorder and uncertainty in the atom types.

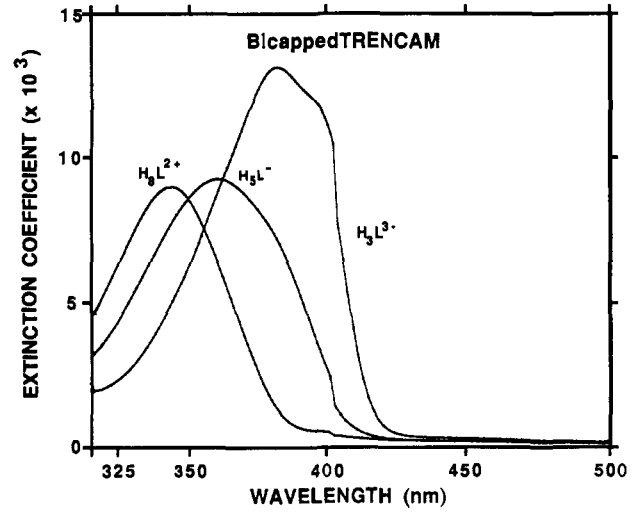

Figure 8. Extinction coefficient spectra generated after refinement of the protonation constants for the bicappedTRENCAM ligand.

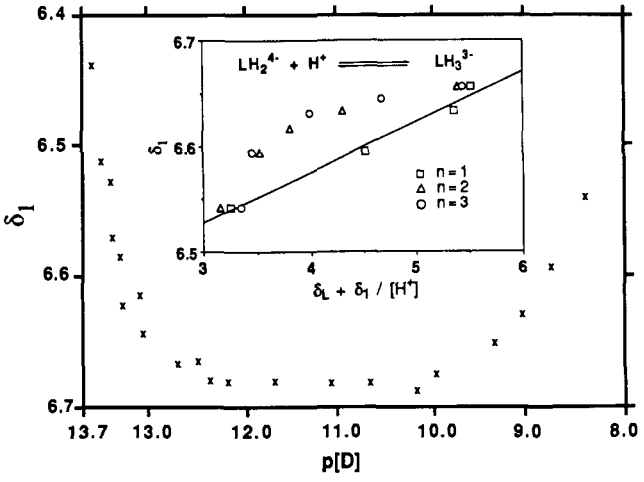

Figure 9. Plot of δ_1 (ArH) versus p[D] for the NMR titration of the bicappedTRENCAM ligand. [Inset is a plot of δ_1 versus $(\delta_L - \delta_1)/[H^+]^n$ for the NMR titration of bicappedTRENCAM. This plot is linear only for $n = 1$. The slope gives an estimate of the log equilibrium constant = 8.3.]

(Figure 7). This plot was linear only for a two-proton step and gave a value for the log protonation constant of 8.7. Schwarzenbach plots on the second buffer region were inconclusive, and the correct model was determined by factor analysis methods.

Refinement of the entire data set was performed with a three-component model relating the species by a two- and then a three-proton step. This model gave R factors $\leq 0.7\%$. The results, based on a weighted average of the two titrations gave the results shown in Table V and extinction coefficient spectra in Figure 8. BicappedTRENCAM was also studied under more basic conditions by examination of the NMR spectra of the protons ArH (δ_1) and $R_2NCH_2CH_2$ (δ_3). Two buffer regions were determined, one at pD > 12 and another at pD < 10 (Figure 9). From pD = 12 to pD = 10 no change was discernible in the NMR spectra. Because of the linear relationship between concentration and chemical shift

$$\delta_{obs} = \delta_L[L]/[L_T] + \delta_{LH_n}[LN_n]/[L_T]$$

a relationship analogous to Schwarzenbach's equation for absorbance data[47] can be obtained.

$$\delta_{obs} = (\delta_L - \delta_{obs})/K[H^+]^n + \delta_{LH_n}$$

For a known δ_L a plot of $(\delta_L - \delta_{obs})/[H^+]^n$ vs δ_{obs} will be linear only for the correct value of n (the number of protons involved in the equilibrium). The slope will be $1/K$ and the intercept will be δ_{LH_n}.

Plots of $(\delta L - \delta_1)/[H^+]^n$ vs δ_1 for the equilibrium at pD < 10 were linear only for a one-proton step (inset, Figure 9). The slope gave a value for the log equilibrium constant of 8.3. Refinement of this model gave an R factor of 0.05%. The equilibrium constant was refined to 8.3 (1).

The correct model for the equilibrium involved at the higher pD (>12) was determined by statistical methods. Refinement yielded an equilibrium constant for the two-proton step of 27.2 (1) with an R factor of 0.18%.

We have, therefore, the protonation equilibria for the bicappedTRENCAM ligand shown in Table V. These results are surprising for several reasons. The primary one is that the average protonation constant = 6.7, which is extremely low. The average value predicted by triethanolamine and 2,3-(dihydroxyethyl)-terephthalamide is 8.4. For most catechols deprotonation does not occur below pH 6.5,[35] but this compound has five deprotonations that occur below pH 4.5! Another interesting result is the number of polyprotic steps. Most tricatechoyl amides protonate in single proton steps. That bicappedTRENCAM has three equilibria with two or more protonations which are unresolved (or simultaneous) demonstrates an unusual degree of cooperativity and implies the presence of important conformational changes concomitant with protonation state.

Metal Complex Studies. Electrochemical Results. Comparison of the reduction potentials for the macrobicycles to previously studied compounds yields the results shown in Table VI. The reduction potentials for this series of ligands are all highly negative. Thus the selectivity for Fe(III)/Fe(II) has been retained in the macrobicyclic series. Note, however, that ratios of K_f vary by only 1.4 orders of magnitude within the macrobicyclic series. This is a very small variation given the stability constant magnitudes. Also interesting is that all tripodal ligands have ratios greater than the bicapped compounds. This may be due to a greater relative stability of the ferrous complex brought on by the bicyclic ligand structure topology. What is perhaps the most surprising, however, is that the larger changes in reduction potential are not between tripods and macrobicycles but between TRENCAM and enterobactin and between bicappedTRENCAM and bicappedTPTCAM. Obviously, effects other than simple cryptate effects are

Table V. Solution Thermodynamic Results for Fe(bicappedTRENCAM)[a]

no. of H+	product species	equilibrium constant	log values	pH at midpoint
2	LH_2	K_1K_2	27.2 (1)	13.6
1	LH_3	K_3	8.3 (1)	8.3
2	LH_5	K_4K_5	8.73 (1)	4.37
3	LH_8	$K_6K_7K_8$	9.75 (1)	3.25
2	MLH_2	K_1K_2	10.65 (1)	5.33
stability constant, ferric complex	ML	K	43.1 (4)	
pM[b]			30.7	

[a] Stepwise protonation constants correspond to the single protonation reactions resulting in the product species shown. For multiple protonation reactions it is the product of the indicated protonation reactions that is determined. [b] Where pM = −log [M] at pH 7.4 and $[M]_T = 10^{-6}$ M, $[L]_T = 10^{-5}$ M.

Table VI. Electrochemical Results

ligand	E°-($Fe^{III}L/Fe^{II}L$) vs NHE	log K_fIII/K_fII	apparent no. of protons transferred	pK_a
MECAM	−1.07	31.2	2.2	9.5
TRENCAM	−1.04	30.6	0.69	11.2
enterobactin	−0.99	29.8	1.00	10.4
TPTCAM	−0.98	29.7	0.52	11.0
bicappedTRENCAM	−0.97	29.5	0.36	11.0
bicappedTPTCAM	−0.92	28.6	0.62	10.3
bicappedTPTTRENCAM	−0.90	28.3	0.59	9.4
bicappedTRENMECAM	−0.90	28.3	0.00	
bicappedTPTMECAM	−0.89	28.1	0.46	11.0

(47) Schwarzenbach, G.; Schwarzenbach, K. *Helv. Chim. Acta* **1963**, *46*, 1390.

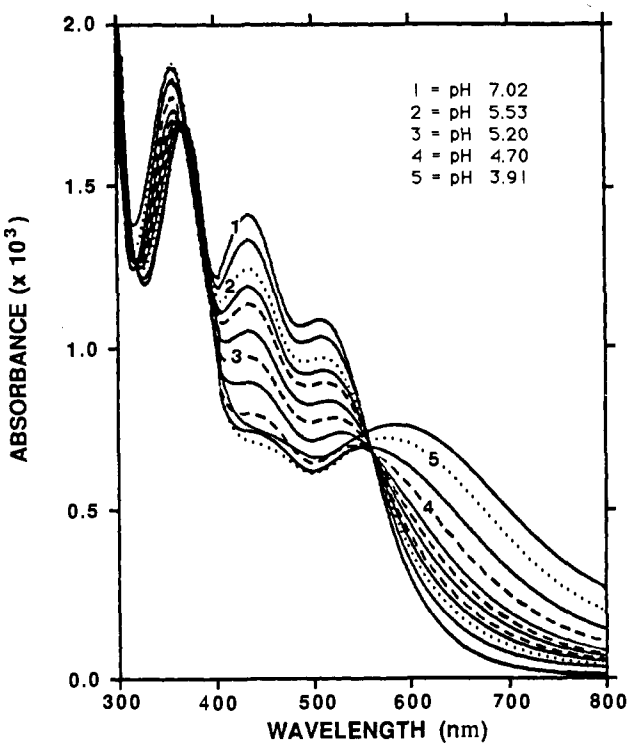

Figure 10. Family of spectra generated by titration of the Fe(bicappedTRENCAM) complex. The concentration of the ferric complex is approximately 20 μM at a constant ionic strength of 0.1 M (KCl).

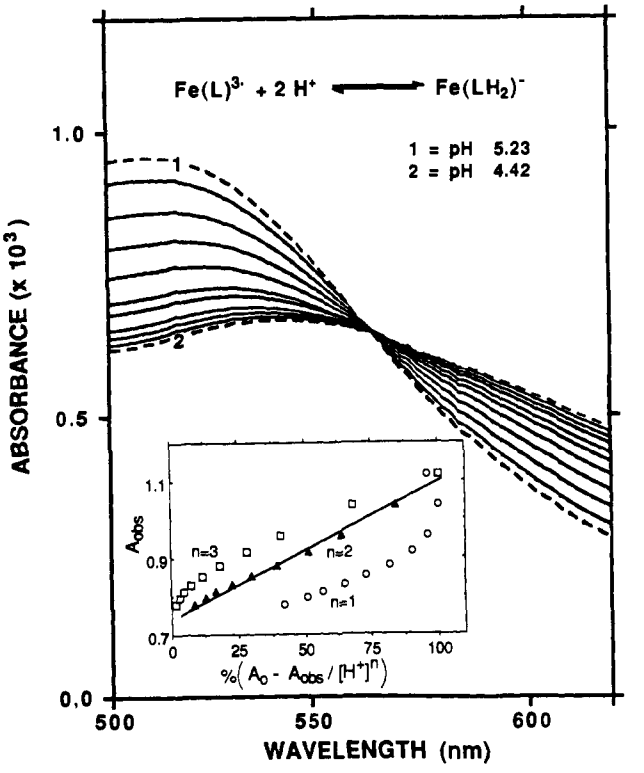

Figure 11. Isosbestic region by titration of the Fe(bicappedTRENCAM) complex. [Inset is a plot of A_{obs} versus $(A_o - A_{obs})/[H^+]^n$ which is only linear for $n = 2$. The slope gives an estimate of the log equilibrium constant = 10.7.]

operative in affecting the selectivities. This is especially important since TPT and TREN are three carbon homologs and, aside from lipophilicity and cavity size, are identical.

Another unusual electrochemical result is the dependence of reduction potential on the pH. At certain pH's protonation of the $Fe^{II}L$ species occurs upon reduction. Surprisingly, in the 85-ms time scale of the experiment a time dependent and therefore nonstoichiometric protonation took place. We presume the nondiffusion-controlled behavior is due to a reorganization of the iron complex upon reduction that is slow on this time scale. Since this slow reorganization does not happen for enterobactin but does occur for compounds with tertiary amines and since the data do not show a demarcation between tripods and macrobicycles, this may not be a macrobicyclic effect but is presumably coupled to inversion of the tertiary amine. Park has shown that inversion equilibria in macrobicyclic bridgehead amines can be observed in this time scale at room temperature.[45]

Metal Complex Protonation. The protonation behavior of the Fe(bicappedTRENCAM) complex was studied by spectrophotometry from pH 11 to pH 3. The family of spectra generated (Figure 10) showed one buffer region between pH 8.3 and pH 3.5. As shown in Figure 11 this buffer region demonstrates isosbestic behavior indicating the presence of only two species in solution. The raw data for the isosbestic region were analyzed by means of a Schwarzenbach plot[47] which was linear only for a two-proton step and yielded a value for the log equilibrium constant of 10.7 (inset, Figure 11). Componentization and refinement with the REFSPEC least-squares program was performed by using a model consisting of one two-proton step.

$$ML + 2H^+ \leftrightarrow MLH_2$$

The R factors for multiple refinements were all $\leq 1.3\%$. The equilibrium constant was determined by weighted average of three refinements to be 10.65 (1) (extinction coefficient spectra are shown in Figure 12).

This behavior is quite similar to ferric enterobactin, which also has its first protonation near pH 5.[48] Unlike the enterobactin

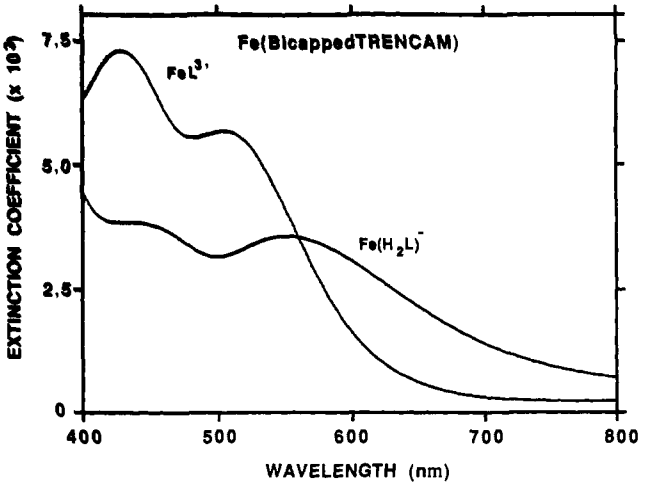

Figure 12. Extinction coefficient spectra calculated after refinement of the protonation constant of Fe(bicappedTRENCAM).

or tripodal analogues, protonation of Fe(bicappedTRENCAM) does not occur stepwise. The change to a salicylate mode of bonding, which is the cause of the single-proton reactions of enterobactin and its tripodal analogues,[49] appears to be sterically inaccessible in the bicappedTRENCAM complex.

Lowering the pH below 3.5 produces a precipitate (presumably MLH_3^0). Due to this precipitation we were unable to ascertain any further protonation behavior by the spectrophotometric method.

Competition Experiments. Because the Fe(bicappedTRENCAM) complex precipitates from solution prior to metal decorporation, the formation constant was determined by competition with CDTA (a stronger ligand than EDTA).[50] The equilibrium

$$FeL + L' \leftrightarrow FeL' + L$$

(48) Harris, W. R.; Raymond, K. N.; Weitl, F. L. *J. Am. Chem. Soc.* **1981**, *103*, 2667.

(49) Cass, M. E.; Garrett, T. M.; Raymond, K. N. *J. Am. Chem. Soc.* **1989**, *111*, 1667.

Table VII. Selected Formation Constants and pM Values[a] for Iron(III) Sequestering Agents

ligand	log K_f	pM[b]
enterobactin	~50	33.5
HBED	39.7	31.0
bicappedTRENCAM	43.1	30.7
MECAM	46	29.1
TRENCAM	43.6	27.8

[a] Values taken or calculated from this work, refs 4 and 5, and the following: Martell, A. E.; Smith, R. M. *Critical Stability Constants*; Plenum: New York, 1976 and 1982; Vols. I–V. [b] Where pM = −log [M] at pH 7.4 and 10^{-6} M $[M]_T$, 10^{-5} M $[L]_T$.

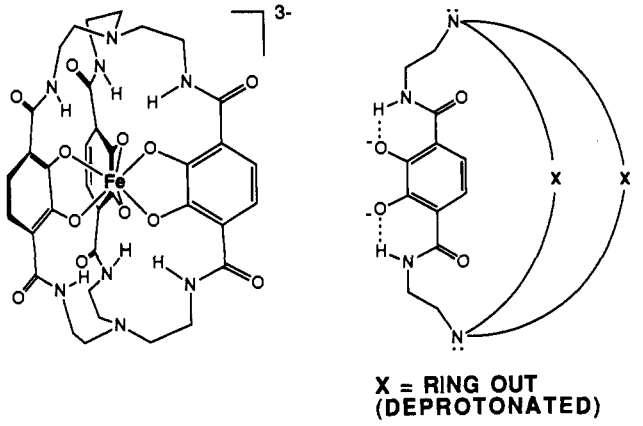

Figure 13. Proposed conformations of the bicappedTRENCAM ligand before and after complexation of the ferric ion.

where L = bicappedTRENCAM and L′ = CDTA was established for five different pH values. Equilibrium took approximately 240 h to be reached. This is at least 5–10 times greater than previous experiments with enterobactin or MECAM and reflects the kinetic chelate effect of the bicyclic ligand structure. The competition equilibrium K_{eq} is given by

$$K_{eq} = \{[FeL'][L]/[FeL][L']\} = K_f(FeL')/K_f(FeL)$$

The concentrations of the species in the above equation may be calculated by measurement of A_{obs} and p[H^+] and the mass balance equations. The value of log K_f (Fe(bicapped TRENCAM)) was determined to be 43.1 (4). In view of the macrobicyclic structure, this value is surprisingly low (Table VII). It is less than that calculated for the related tripodal ligand TRENCAM, suggesting (1) an absence of a macrobicyclic effect and (2) an absence of ligand preformation for iron binding. These results parallel related siderophore analogues,[12,51] where the formation constants show little or no dependence on the ligand topology, implying that enthalpy is the dominant factor in iron complexation compared with reorganization entropy.[52] The free energy of coordination of ferric ion by anionic oxygen atoms, the type of donor group found in the catechol ligand, is dominated by the enthalpy of charge neutralization.[52,53] The relative enthalpy and entropy changes accompanying structural changes of enterobactin[52] or its analogues[54] are consistent with this. The lack of a macrobicyclic effect may be due to a free ligand conformation where all three binding subunits have swung out of the cavity to maximize the solvation energy (Figure 13).

These results are not consistent with the report by Vögtle et al.[11] of a stability constant of 10^{59}, which would represent a macrobicyclic effect of 13 orders of magnitudes. The redox potentials for the series of bicapped macrocyclic iron complexes are all nearly the same, indicating similar stability constants. Therefore the stability constant for the macrocyclic ligand of Vögtle et al. is most probably near 10^{43} rather than 10^{59}.

Unlike the formation constant of bicappedTRENCAM, the pM value (30.7) is relatively large. Since this is a direct thermodynamic measurement of a ligand's ability to complex the metal ion at physiological pH, this value shows bicappedTRENCAM to be the strongest synthetic iron chelating agent produced by this laboratory (Table VII). This is a reflection of this ligand's dramatically lower pK's coupled with only a three order of magnitude drop in formation constant from MECAM. This result of an excellent pM value parallels the results found for the binding subunit[15] and again suggests the importance of enthalpy as a dominant consideration in the metal binding process of catechol ligands.

Conclusions

This paper has reported the synthesis of a general series of macrobicyclic iron(III) sequestering agents. Five new ligands have been synthesized with a systematic variation in cavity size, flexibility, charge, and solubility. A high-yield template synthesis has been demonstrated. This route dramatically simplifies the synthesis of these compounds, which involve the formation of six amide bonds. Voltammetry of the ferric complexes has shown that selectivity for the ferric ion has been retained, but that the only macrobicyclic effect discernible is a slight stabilization of the ferrous complex relative to the ferric. A novel nondiffusion-controlled protonation of the ferrous complexes is found which is presumably due to a slow molecular reorganization upon reduction. Solution thermodynamic studies have demonstrated the presence of surprisingly low ligand protonation constants, and a novel degree of cooperativity in forming a number of polyprotic steps. The protonation behavior of the ferric complex proceeds in an unusual two-proton step, apparently without forming a salicylate mode of bonding. The value of the formation constant, determined to be 10^{43}, shows an absence of a macrobicyclic effect. The pM value of 30.7 is the highest for any of the siderophore analogues we have prepared and reflects a combination of high formation constant with low protonation constants. The structural characterization of Fe(bicappedTRENCAM) represents the first analysis of a hexadentate catechol complex analogous to enterobactin and demonstrates the first trigonal prismatic coordination geometry found for the Fe^{3+}.

Acknowledgment. We thank Dr. Frederick J. Hollander (for his help with the crystallography), Dr. Scott Rocklage of Salutar, Inc. (for a gift of CDTA), and Dr. Dan Stack for helpful discussions. This research was supported by NIH Grant DK32999. Partial postdoctoral fellowship support from the NIH (to T.J.M.) and NATO postdoctoral fellowships (to M.W.H. and F.E.H.) are gratefully acknowledged.

Registry No. **1**, 75956-64-8; **2**, 131933-29-4; **3**, 131973-28-9; **4**, 131933-30-7; **5**, 107712-28-7; **6**, 131933-31-8; **7**, 110354-51-3; **8**, 131933-32-9; **9**, 110354-54-6; **10**, 110354-55-7; **11**, 110354-56-8; **12**, 131933-33-0; **13**, 131933-34-1; **14**, 131933-35-2; **15**, 131933-36-3; **16**, 18226-42-1; **17**, 107864-71-1; **18**, 77372-56-6; **19**, 131851-93-9; **20**, 131933-37-4; **21**, 131851-95-1; **22**, 107712-29-8; **23**, 131972-93-5; **24**, 110453-91-3; **25**, 107712-27-6; TREN, 4097-89-6; TPT, 4963-47-7; FeCDTA, 52305-99-4; [Fe(bicappedTRENCAM)]$^{3-}$, 107712-33-4; [Fe(MECAM)]$^{3-}$, 69058-77-1; [Fe(TRENCAM)]$^{3-}$, 131933-38-5; [Fe(enterobactin)]$^{3-}$, 61481-53-6; [Fe(TPTCAM)]$^{3-}$, 131933-39-6; [Fe(bicappedTPTCAM)]$^{3-}$, 131972-94-6; [Fe(bicappedTPTTRENCAM)]$^{3-}$, 131972-95-7; [Fe(bicappedTRENMECAM)]$^{3-}$, 110372-01-5; [Fe(bicappedTPTMECAM)]$^{3-}$, 131973-29-0; benzyl chloride, 100-44-7; dimethyl 2,3-dihydroxyterephthalate, 75956-62-6; *N*-hydroxysuccinimide, 6066-82-6.

Supplementary Material Available: Derivations of equations used in electrochemical analysis, X-ray structure material con-

(50) Martell, A. E.; Smith, R. M. *Critical Stability Constants*; Plenum: New York, 1974; Vol. 1, p 236.

(51) Sun, Y.; Martell, A. E.; Motekaitis, R. J. *Inorg. Chem.* **1986**, *25*, 4780.

(52) Scarrow, R. C.; Ecker, D. J. Chiu, N.; Liu, S.; Raymond, K. N. *Inorg. Chem.*, in press.

(53) Phillips, C. S. G.; Williams, R. J. P. *Inorganic Chemistry*; Oxford University Press: Oxford, 1965; Vol. 1, p 161.

(54) Garrett, T. M.; Cass, M. E.; Raymond, K. N., submitted for publication.

tained in tables of atom positional parameters, least squares planes, and anisotropic thermal parameters, and solution thermodynamic material contained in figures of observed and calculated dependent variables for the spectrophotometric titration of the bicapped-TRENCAM ligand, observed and calculated chemical shifts for the NMR titration of the bicappedTRENCAM ligand, observed and calculated dependent variables for spectrophotometric titration of the Fe(bicappedTRENCAM) complex, and plot of absorbance vs time for the competition experiment with CDTA and Fe(bicappedTRENCAM) (13 pages); table of observed and calculated structure factors (13 pages). Ordering information is given on any current masthead page.

Spectroscopic Studies of the Electronic Structure of Iron(III) Tris(catecholates)

Timothy B. Karpishin,[†] Matthew S. Gebhard,[§] Edward I. Solomon,*[,§] and Kenneth N. Raymond*[,†]

Contribution from the Department of Chemistry, University of California, Berkeley, California 94720, and Department of Chemistry, Stanford University, Stanford, California 94305. *Received August 31, 1990*

Abstract: Single-crystal polarized absorption and magnetic circular dichroism (MCD) have been employed to elucidate the electronic structure of the iron(III) tris(catecholate) complex $[Fe(cat)_3]^{3-}$ to investigate the bonding in ferric enterobactin and similar catechol siderophores. In addition to $[Fe(cat)_3]^{3-}$, two related complexes, $[Fe(TRENCAM)]^{3-}$, a catecholamide, and $[Fe(eta)_3]^{3-}$, a terephthalamide, have been studied by MCD to provide a perturbation on the electronic structure of $[Fe(cat)_3]^{3-}$ and to also determine differences in bonding between the three complexes. The ligand-to-metal charge-transfer (CT) band characteristic of the catecholate siderophores is found for $[Fe(cat)_3]^{3-}$ to be composed of two overlapping x,y polarized transitions at 18414 and 22018 cm^{-1}. These transitions are ligand π to metal d in nature; assignments of these and four other CT transitions and an experimental energy order for the molecular orbitals of the complexes are made in D_3 symmetry. It is evident from analysis of the spectra that a significant contribution to the Fe–O interaction in these complexes is made by π bonding. An estimate of $10Dq$ as ~ 13000 cm^{-1} is made for the iron(III) tris(catecholates) from the transition energy of the spin forbidden ligand field $(LF)^6A_1 \rightarrow {}^4T_1$ transition observed in the MCD. A value of $10Dq$ is also obtained from the CT transition energies and is determined to be $\sim 63\%$ of the value obtained from the LF transitions. This reduction indicates that the CT excited state is best described as an iron(II) species. Analysis of the CT spectra indicates that the electronic structure of the two complexes $[Fe(cat)_3]^{3-}$ and $[Fe(TRENCAM)]^{3-}$ are similar, whereas $[Fe(eta)_3]^{3-}$ shows a higher degree of σ and π interactions in Fe–O bonding. The contribution of differences in bonding to the known thermodynamic stability constants is discussed.

In response to the challenge posed by iron requirement and unavailability, microorganisms secrete high-affinity iron-binding compounds called siderophores.[1-4] The siderophores are powerful chelating agents which typically use hydroxamate (R–N(O^-)C(O)–R′) or catecholate groups to coordinate the ferric ion octahedrally. The characterization of the physical properties of siderophores and their synthetic analogues are of interest because of their high selectivity for iron(III), and in the case of the tris(catecholates), their remarkable thermodynamic stability ($K_f > 10^{40}$).[5] One striking characteristic of these iron complexes is their intense red color (the original name siderochrome referred to this color), which is attributable to spin-allowed ligand-to-metal charge-transfer (CT) transitions. Although the CT spectra of the siderophores and their analogues have been used extensively as fingerprints to measure stability constants,[5-7] to follow the kinetics of Fe removal from transferrin,[8] and to elucidate protonation behavior,[9] a detailed assignment of the observed transitions has not appeared. The visible spectra of the tris(hydroxamate) (e.g., ferrichrome A) and the tris(catecholate) (e.g., enterobactin) siderophores are generally dominated by one broad intense band at 20000–22000 cm^{-1}.[1,10] The similarity between these visible spectra would indicate common features for the electronic structure of these chromophores. The goal of this study is to elucidate the electronic structure in iron(III) tris(catecholates) and thus determine the contribution of the electronic structure to the high-affinity bonding in the catecholate siderophores.

The iron(III) tris(catecholate) complex, $[Fe(cat)_3]^{3-}$, is a simple model for ferric enterobactin[11,12] (Figure 1) having a similar visible spectrum[13] and also very high thermodynamic stability.[5,14] Although assignment of the CT bands in $[Fe(cat)_3]^{3-}$ has been previously addressed,[13] there has been only one thorough study of the electronic structure of the complex.[15] The authors of the

[†] University of California, Berkeley.
[§] Stanford University.

(1) Matzanke, B. F.; Müller-Matzanke, G.; Raymond, K. N. In *Iron Carriers and Iron Proteins*; Loehr, T. M., Ed.; Physical Bioinorganic Series; VCH Publishers: New York, 1989; pp 1–121.
(2) Raymond, K. N.; Carrano, C. J. *Acc. Chem. Res.* **1979**, *12*, 183.
(3) Raymond, K. N.; Müller, G.; Matzanke, B. F. *Top. Curr. Chem.* **1984**, *123*, 49.
(4) Neilands, J. B. *Ann. Rev. Biochem.* **1981**, *50*, 715.
(5) Avdeef, A.; Sofen, S. R.; Bregante, T. L.; Raymond, K. N. *J. Am. Chem. Soc.* **1978**, *100*, 5362.
(6) Harris, W. R.; Carrano, C. J.; Cooper, S. R.; Sofen, S. R.; Avdeef, A. E.; McArdle, J. V.; Raymond, K. N. *J. Am. Chem. Soc.* **1979**, *101*, 6097.
(7) Garrett, T. M.; Miller, P. W.; Raymond, K. N. *Inorg. Chem.* **1989**, *28*, 128.
(8) Kretchmar, S. A.; Raymond, K. N. *J. Am. Chem. Soc.* **1986**, *108*, 6212.
(9) Cass, M. E.; Garrett, T. M.; Raymond, K. N. *J. Am. Chem. Soc.* **1989**, *111*, 1677.
(10) Raymond, K. N.; Abu-Dari, K.; Sofen, S. R. In *Stereochemistry of Optically Active Transition Metal Compounds*; Douglas, B. E., Saito, Y., Eds.; ACS Symposium Series No. 119; American Chemical Society: Washington, DC, 1980; pp 133–167.
(11) Anderson, B. F.; Buckingham, D. A.; Robertson, G. B.; Webb, J.; Murray, K. S.; Clark, P. E. *Nature* **1976**, *262*, 722.
(12) Raymond, K. N.; Isied, S. S.; Brown, L. D.; Fronczek, F. R.; Nibert, J. H. *J. Am. Chem. Soc.* **1976**, *98*, 1767.
(13) Salama, S.; Stong, J. D.; Neilands, J. B.; Spiro, T. G. *Biochemistry* **1978**, *17*, 3781.
(14) Loomis, L. D.; Raymond, K. N. *Inorg. Chem.*, in press.
(15) Gordon, D. J.; Fenske, R. F. *Inorg. Chem.* **1982**, *21*, 2916.

0002-7863/91/1513-2977$02.50/0